Chapter 12

QUANTUM NUCLEAR DYNAMICS OF THE H_3^+-SYSTEM AND ITS ISOTOPOMERS

Ralph Jaquet

Theoretische Chemie, Universität Siegen, D-57068 Siegen, Germany

theo@theo.chemie.uni-siegen.de

1. Introduction

H_3^+ was discovered by Thomson, 1911 [1], and Coulson, 1935 [2] predicted the equilibrium structure of H_3^+ (for the electronic singlet state) to be an equilateral triangle with a bond length of 1.61 a_o (0.85 Å) quite close to the modern value of 1.6500 a_o [3, 4]. With the advent of computers, this prediction was confirmed and the stability of the non-classical three-center, two- electron bond was established (Cristofferson *et al.* 1964 [5]; Conroy 1964 [6]). From the early theoretical work it was soon evident that H_3^+ has no stable electronically excited singlet state and its only sharp spectrum would be the vibration-rotation spectrum in the infrared (Carney and Porter, 1976 [7]; Watson, 1984 [8, 9]; Sutcliffe and Tennyson, 1987 [10]). The detection of H_3^+ had to await the age of laser spectroscopy (Oka, 1980 [11]).

H_3^+ is the simplest and most fundamental polyatomic molecule, consisting of only three protons and two electrons. As such, it plays important roles in the laboratory spectroscopy [12] of hydrogen-rich plasmas, the theoretical calculations of rotation-vibrations energy levels, and the theoretical and experimental investigations of collisions of $H^+ + H_2$, $H_2^+ + H_2$, needed to understand the chemistry of interstellar clouds.

The relative simplicity of the hydrogen molecular ion H_3^+ makes it a good target for extensive quantum chemical calculations on the highest levels of sophistication. Since it plays an important role in astrophysics [13] and its IR-spectrum has been detected experimentally [11], very accurate calculations have fundamental importance and can stimulate an interplay between theory and experiment similar to the famous case of H_2.

We cannot review here the history of quantum chemical calculations on H_3^+; some details are found in Refs. [14, 15]. The best conventional CI calculation by Meyer, Botschwina, and Burton (MBB), 1986 [16] of the most relevant part of the potential energy surface (PES) represents a first landmark. The points to be calculated were chosen carefully. Agreement with experiment was improved by means of a single adjustable parameter. A next step forward was the paper by Röhse, Kutzelnigg, Jaquet, and Klopper (RKJK), 1994 [17, 18], who applied the R12 method [14, 19, 20] to this problem and obtained an absolute accuracy of a few cm^{-1} along the whole surface (of course, without any semiempirical parameter). It soon became clear that at this level of accuracy corrections beyond the Born-Oppenheimer approximation must no longer be neglected, and it was conjectured [21] that the bulk of the remaining disagreement with experiment should be due to the neglect of adiabatic corrections. In fact, the adiabatic corrections for the H_2 molecule were known to be of the order of 100 cm^{-1}.

The next logical step was therefore the evaluation of (diagonal) adiabatic corrections to the PES, which at SCF level was done by Tennyson and coworkers [22]. The RKJK surface with this approximate adiabatic correction led to a remarkably good agreement with experiment. Nevertheless, as pointed out by the authors of Refs. [21] and [22], experimental data could still be better reproduced by effective potentials of the MBB form, which are based on MBB- or RKJK-parameters, part of which were adjusted to spectroscopic data [23–26]. In these authors' analysis, the results for different isotopomers showed similar systematic errors which didn't exhibit the mass dependence expected for non-BO effects. Of course, one could not exclude that relativistic effects might play a role. These have so far always been neglected. This state of the matter was a challenge for Cencek *et al.*, 1998 [27] to calculate the PES of H_3^+ at a much higher level of accuracy than it has been possible previously and to account for both adiabatic and relativistic corrections.

In several papers [27–30], we reported on *ab initio* calculations of the rovibrational spectrum of H_3^+, based on a "sub-wavenumber" accurate potential energy surface (PES). The PES, that is based on Gaussian Geminals, includes, in addition to the calculations of the electronic contributions to the Born-Oppenheimer (**BO**) -energy, relativistic effects and adiabatic contributions. The remaining deviations we found (if adiabatic corrections have already been included) are of the size of a few tenth of a wavenumber for H_3^+, H_2D^+, and D_2H^+, but much smaller for D_3^+. It was suggested in [27, 28] that the remaining discrepancy is probably due to non-adiabatic contributions which in the case of H_3^+ are supposed to be smaller than in the case of H_2. Results for the simulation of non-adiabatic contributions have been discussed in [29–31], showing deviations to experiment of hundredths of a wavenumber.

The best calculations of the spectrum of H_3^+ have shown that the remaining discrepancies to experiment are related to the missing non-adiabatic corrections. Non-adiabatic corrections have been calculated by us [32] with nearly the same accuracy as the diagonal adiabatic corrections. The fit for the complete surface of the non-adiabatic corrections, coupling at least the three lowest electronic states, is yet not finished, so the calculations for the rovibrational frequencies have been simulated by now using different masses for the individual rotational and vibrational motion of the three nuclei.

What has not been taken care of, is the influence of the Lamb-shift on the potential energy surface, which we expect to be small. A further contribution, which has been neglected so far, is the spin-orbit interaction between the bound electronic singlet and the bound electronic triplet states. No other bound electronically excited states of H_3^+ are known.

First-principles theoretical investigations of spectra of polyatomic molecules are nowadays a formidable task at least for triatomic systems. The deviations between calculated and experimental spectra depends on three different subjects: (a) the solution of the electronic Schrödinger equation, (b) the solution of the nuclear motion problem and (c) the question whether the Born-Oppenheimer Ansatz is appropriate. In the case of few electron systems with few degrees of freedom, converged results can be reached. The absolute accuracy of the frequencies depends on the quality of the potential energy surface: (a) for scattering problems an extended region of the potential energy surface is needed, and consequently the *ab initio* calculation are mostly of inferior accuracy and (b) in case of spectroscopy a smaller local region of the potential energy surface is probed. The experimental work of Carrington, McNab *et al.* [33–35] on the spectroscopy near the dissociation limit is a demanding problem for a theorist.

H_3^+, a benchmark molecule for theorists [14–17, 36, 37], shows unusual spectroscopic effects [13, 34]. Because it is a fairly floppy molecule (there is the *IR* inactive 'breathing' mode $\nu_1(A_1)$ and the double degenerate *IR* active $\nu_2(E)$ mode), it undergoes large-amplitude vibrational motions to such extent that the rovibrational spectrum does not conform to many of the standard rules of spectroscopy. The first fifteen lines of the ν_2 fundamental band were originally observed by Oka [11] in 1980, close to earlier *ab initio* predictions of Carney and Porter [7, 38]. While no electronic spectrum of H_3^+ has been observed experimentally, several theoretical investigations of the potential energy surfaces of the electronic triplet H_3^+ and its rovibronic states [39,40] have been performed recently.

There has been much work in the literature to provide potential energy surfaces needed for spectroscopic and/or scattering ($H^+ + H_2$) problems. Since the MBB-work [16], based on Full-CI calculations near equilibrium geometry, there have been several very accurate electronic structure calculations for local [27,28,37,41] and global [41–43] potential energy surfaces. Numerous global surfaces are available, created by adjusting *ab initio* data with respect to experimental information [42,44–46] and using the 'diatomics in molecules' method (DIM) [43,47–49].

An overview of the astronomy, physics and chemistry of H_3^+ has been presented in [4]. We will present in this overview how the use of explicitly correlated electronic wavefunctions has dramatically improved the quality of (a) the BO-surface and (b) the additional corrections or contributions beyond the BO-ansatz. This results in rovibrational transition frequencies which can be now specified of being of spectroscopic accuracy. Some details of how we fit the *ab initio* data using different methods will be given. We will summarize the quality of the rovibrational eigenvalues and transition frequencies compared to the most recent experimental work of McCall and Oka [50], Lindsay and McCall [51,52] on fundamental and, as well, combination band spectroscopy of H_3^+ together with the most recent evaluation and compilation of the laboratory spectroscopy of H_3^+. We will review the present status of agreement and disagreement between theory and experiment, the latest results coming from Born-Oppenheimer approaches and how the inclusion of relativistic, adiabatic and non-adiabatic effects will modify the results. We will analyze the quality of the potential energy surface fitting, possible choices of coordinates for the fitting and the different aspects of how variational calculations for the nuclear motions can be performed.

2. Analytical fit of the electronic structure data: potential energy surfaces, relativistic, adiabatic and non-adiabatic corrections

The basis for molecular dynamics investigations (scattering, spectroscopy, *etc.*) is the knowledge of the interaction potential, either in the form of a full multidimensional hypersurface (PES) or in the form of single values for the potential and its derivatives at special values of the coordinates. If a hypersurface is needed, one can use fitting functions that perform well in a local region, or one has to use global functions that cover a large range with “fairly good” accuracy. For local approximations, one frequently uses interpolating functions (splines), expansions in polynomials or rational functions, *etc.* Functional forms that are special and simulate a special topography of the PES (*e.g.* Morse functions, separation of the many body potential into two-body, three-body, *etc.* interactions) are used for both local and global interpolations. An overview about typical "fitting problems" has been given in the literature [53–59]; new general approaches that have been used in case of H_3^+ are those of Aguado and Paniagua *et al.* [43] and Ho *et al.* [60].

A very detailed analysis for the local region around the minimum has been performed by Burton *et al.* [61], They have analyzed a power series expansion in the sixth order (23 parameters) for 78 energy points and used three different types of coordinates, namely Dunham, Simons-Parr-Finlan (SPF) and Ogilvie type variables in the internuclear distance. In addition to their large differences in the rms-values, an energy contour plot revealed big differences for the three types of expansions, even when similar rms-values suggest comparable quality of the fit.

Meyer, Botschwina, and Burton (MBB) [16] presented in their work a prescription on how to choose points around the potential energy minimum in order to achieve a high accuracy in fitting the *ab initio* energy points to a functional ansatz for the PES. In our recent work on highly accurate PESs, which have been calculated with the CI-R12 [17] and Gaussian Geminals [27,28] method, we started with exactly the 69 points of the PES chosen according to the prescription of MBB [16]. The points have been labeled by three integers n_a, n_x, and n_y, which are related to the Morse-type symmetry adapted deformation coordinates (MSADC) S_a, S_x, and S_y

$$S_a = 0.15 n_a = (\tilde{R}_{12} + \tilde{R}_{13} + \tilde{R}_{23})/\sqrt{3} \tag{12.1}$$

$$S_x = 0.15 n_x = (2\tilde{R}_{12} - \tilde{R}_{13} - \tilde{R}_{23})/\sqrt{6} = S_e \cos\phi \tag{12.2}$$

$$S_y = 0.15 n_y = (\tilde{R}_{23} - \tilde{R}_{13})/\sqrt{2} = S_e \sin\phi, \tag{12.3}$$

with

$$\tilde{R}_{kl} = \frac{1}{\beta}\left\{1 - \exp\left[-\beta\left(\frac{R_{kl}}{R_{\mathrm{ref}}} - 1\right)\right]\right\}, \quad \beta = 1.3, \quad R_{\mathrm{ref}} = 1.65 \text{ bohr} \tag{12.4}$$

The 69 points define a part of the whole PES from the minimum up to well above the barrier to linearity. The functional form is chosen such that it can be used up to the asymptotic region (H^+ + H_2, H+H+H^+), but the most reliable part includes the energy-region up to $\approx$ 20000 cm^{-1} above the minimum.

Except for the work of Carrington *et al.* [33–35] on the infrared predissociation spectroscopy of H_3^+, all experiments have been performed for rovibrational transitions, which probe the part of the PES below the barrier to linearity. In our opinion, the quality of the available highly accurate PESs is limited to the region slightly above the barrier to linearity. Those other PESs described in the literature which cover the whole energy region are satisfying mostly the demands of scattering calculations.

In the most recent work [30] we report on an extension of our PES using additional points coming from the same prescription as given in Eqs. (12.1-12.4), but taking nearly all possible integers values for n_a, n_x, and n_y, which fulfill the triangle inequality for the three internuclear distances. Former calculations have shown that the contributions of at least the adiabatic diagonal corrections are needed for precise predictions of rovibrational frequencies. In [30] the range of the calculated points on the ground state PES has been extended to cover an energy region up to 40000 cm^{-1} above the minimum and adiabatic diagonal corrections have been included in all parts of the PES.

Whereas the fitting of the minimum region of the PES is relatively straightforward, an appropriate description of the PES far beyond the minimum, showing the proper symmetry, is less easy. The aspect of the existence of undesirable structures and lack of symmetry (especially for a homonuclear triatomic molecule) is discussed in the work of Aguado *et al.* [43]. Some of the most recent works on H_3^+ (electronic singlet state) report about calculations of a much larger set of data to produce a global surface which is based on, (a) less accurate electronic structure methods [62], (b) combination of highly accurate with less accurate data [41,43] or (c) additional empirical functional forms which represent the asymptotic part of the surface well [41]. Investigations of the electronic triplet state of H_3^+ are increasing [39, 40] and already rovibrational calculations have been performed [40].

2.1 Polynomial fit

In the case of a polynomial expansion, the fit for the system H_3^+ (and its isotopomers) has been performed in three different ways:

1 The electronic energies, relativistic and adiabatic contributions are added up for each point, and a power series expansion in MSADC (Eqs. 12.1-12.4) is performed for the full potential V using different orders N_{max}

$$V = \sum_{n,m,k} V_{n,m,k} S_a^n S_e^{m+k} cos(k\phi), \quad n+m+k \leq N_{max} \qquad (12.5)$$

2 Each energy contribution is separately fitted to a power series expansion using MSADC, and all parts are added up.

3 The electronic energy and the relativistic contribution are added up and fitted to a power series expansion using MSADC. The adiabatic corrections are fitted *mass-independently* in MSADC or the original SADC (Eqs. 12.1-12.3, with the $\tilde{R}_{kl}$ as interatomic distances).

Each contribution to the total potential energy can be described by a different coordinate expansion.

2.1.1 Results of the fit with CI-R12. In the CI-R12 method of Kutzelnigg and coworkers [19, 63, 64] the electronic wavefunction is approximated as

$$\Psi(1,2) = c_0 r_{12} \Phi^0(1,2) + \sum_{l=1}^{max} c_l \Phi_l(1,2), \qquad (12.6)$$

where the $\Phi_l(1,2)$ are two-electron singlet Slater determinants and r_{12} is the inter-electronic distance. The reference wavefunction $\Phi^0(1,2)$ is a singlet Slater determinants built from molecular orbitals corresponding to the lowest eigenvalue of the reference Hamiltonian, which is the bare nuclear Hamiltonian that has turned out superior to the self-consistent field reference. In the earliest calculations [14] the convergence with the size of the basis set has been studied, so that for the evaluation of the PES, the basis $16s10p8d$ contracted to $10s8p6d$ seemed to be sufficient [17]: 69 points, with energies up to 23000 cm^{-1} above zero (*i.e.* potential energy minimum), had been calculated (called CIR12*d*). In Ref. [17] a few points are presented that had been calculated including f-functions in the basis set (recent calculations have shown that a considerable improvement can be gained for configurations further away from the minimum [41]).

2.1.2 Results of the fit with Gaussian Geminals. In the case of the Gaussian Geminals method at first 69 points around the minimum region had been available [27]; further points will be calculated, and several additional points in the asymptotic region are already available. The ansatz for the electronic wave function

$$\Phi = \sum_{i=1}^{K} c_i \phi_i, \tag{12.7}$$

$$\phi_i = (1 + P_{12}) \exp\left(-\alpha_{1i}|\boldsymbol{r}_1 - \boldsymbol{A}_i|^2 - \alpha_{2i}|\boldsymbol{r}_2 - \boldsymbol{B}_i|^2 - \beta_i r_{12}^2\right) \tag{12.8}$$

is described by Rychlewski, Cencek *et al.* [36, 65] (see also Chapter 4 within this book).

The coefficients $V_{n,m,k}$ for the fit are given in Ref. [28] in different variants (see Eqs. (12.1-12.4)) for different isotopomers. If one uses very high order polynomial fits (with nearly as many parameters as input data) the use of singular value decomposition is needed to eliminate linear dependencies. We tested the quality of the fit in different ways to be sure that there are no problems with creating oscillatory behavior of the polynomial expansion in the range of the given 69 points; this problem has been discussed in detail in our earlier work [28]. Nevertheless, Polyansky and Tennyson [31] re-fitted the data, because our procedure did not seem to be reliable or accurate enough for them; but, from results presented in [30, 51], one could guess, that the fit is inferior. The standard deviation of our different fits and energies near the dissociation limit together with the results coming from other fitting procedures, including different *ab initio* data and different set of conformations, are presented in [14, 27, 30]. The weighted root mean square deviation for 7th to 10th order polynomial expansion varies between 1.2 to 0.05 cm^{-1} for the BO-energies. The potential ansatz, presented in Eq. (12.5), is not appropriate for the asymptotic region, if one chooses $\beta = 1.3$, and so a more flexible ansatz as proposed by Prosmiti *et al.* [42], Polyansky *et al.* [41], and Aguado *et al.* [43], has to be used. If one chooses ansatz (12.1-12.5) and wants in addition a better description of the PES beyond the area defined by the 69 points, one simply includes conformations far in the asymptotic region (in our case for $H_2 + H^+$, we took the diatomic data of H_2 from Kołos and Wolniewicz). One gets a global PES which describes the PES in the minimum region and the asymptotic region with high accuracy (this is done by choosing $\beta = 1.$ in Eq. 12.4) with absolute errors in the range of a few wavenumbers. The frequencies calculated from a PES made out of 69 points, with or without including the asymptotic conformations, are in principle the same. The intermediate region is not described 'badly', but is much less accurate than the regions where data are given. Another choice is to use a more flexible ansatz as proposed by Ho and Rabitz [60], Prosmiti *et al.* [42], Polyansky *et al.* [41], and Aguado *et al.* [43], A further possibility is to use a multi-level fit, based on a first fit to a LEPS or DIM potential and where the deviation to the *ab initio* data is fitted additionally, which can be gradually improved by including data of increasing accuracy, depending on the electronic structure method.

Plots of the total energy including electronic, relativistic and adiabatic contributions and the difference of the BO-states between GG and CI-R12 (without f-functions) are presented in Fig. 12.1 and 12.2.

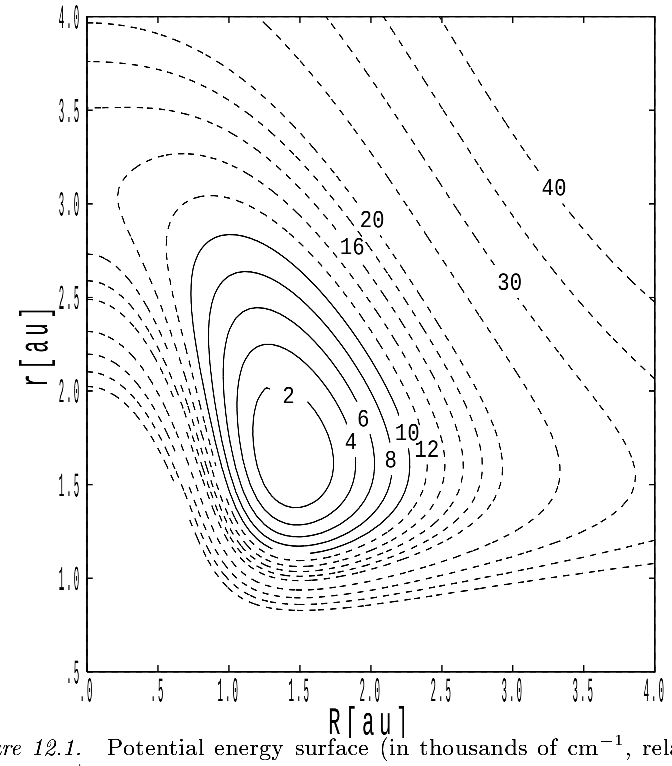

Figure 12.1. Potential energy surface (in thousands of cm^{-1}, relative to the minimum) of H_3^+ (including electronic, relativistic and adiabatic contributions) in Jacobi coordinates for C_{2v}-symmetry [28]. Contours are given in steps of 2000 cm^{-1}. Starting with the 11th line contours are given in steps of 5000 cm^{-1}. The region, where most of the transition frequencies are calculated, is between the bottom of the potential energy surface and the contour 5 (10000 cm^{-1}).

2.1.3 Results of the fit for the combination of CI-R12 and Gaussian Geminals. In the multi-reference CI-R12 Ansatz [66] the electronic wavefunction is approximated as (see for comparison Eq. (12.6))

$$\Psi(1,2) = \sum_{i=1}^{N_0} c_i r_{12} \Phi_i^0(1,2) + \sum_{l=1}^{max} d_l \Phi_l(1,2), \qquad (12.9)$$

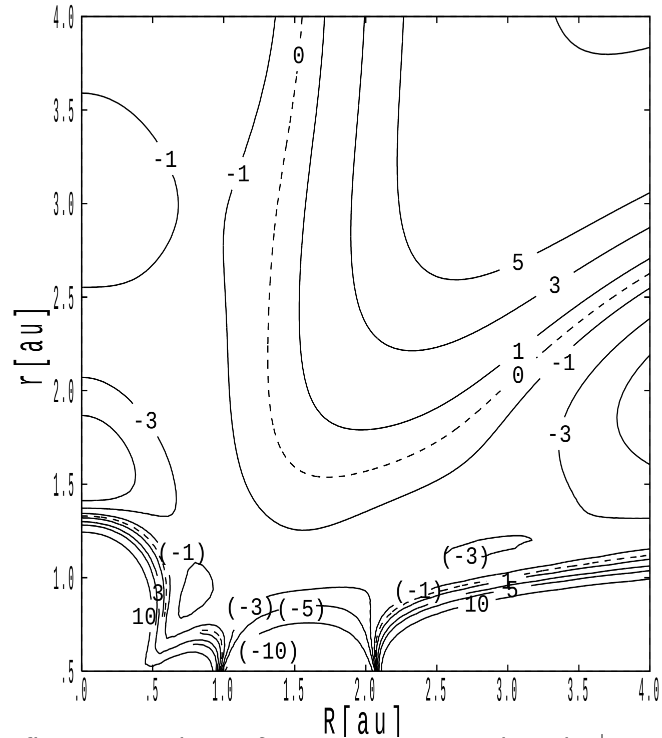

Figure 12.2. Difference-plot of the BO potential energy surface of H_3^+ between GG and CI-R12 [17] (without f functions) [28]. Contours are given in units of cm^{-1}.

where the $\Phi_l(1,2)$ are two-electron singlet Slater determinants and r_{12} is the inter-electronic distance. The reference wavefunctions $\Phi_i^0(1,2)$ are those singlet Slater determinants built from molecular orbitals corresponding to the lowest eigenvalues of the reference Hamiltonian. We have performed in our recent work for several excited states calculations with N_0 up to four [67]. Whereas in earlier calculations [17] for H_3^+ 69 points were included up to 23000 cm^{-1} above zero, we can use now around additional 265 points [67] up to the largest integer value ($n_a^{max} = 8$) in agreement with the prescription given by Eqs. (12.1-12.3). A detailed list of the *ab initio* data for several electronic states [67], together with adiabatic and non-adiabatic corrections [32] will be published soon. For the fit the asymptotic region is excluded because for that part of the PES the functional form given in Eq. (12.5) is not appropriate. We will use these data for investigations of the rovibrational states above the barrier to linearity. The *ab initio* points have been calculated with the same basis set (*i.e.* without f-functions) as the former 69 points as given in [17] (called CIR12d). We can compare our data with the CI-R12 *ab initio* points of W. Klopper (as presented in [41]), who calculated the energy for several additional points using f-functions in the basis (called CIR12f). We have used these two sets of data (CIR12d, CIR12f) and combined them with the GG-points for a new **BO**-fit to get a highly accurate PES up to 40000 cm^{-1} above zero (GGCIR12d, GGCIR12f). If one tries to incorporate configurations of the asymptotic region the polynomial ansatz as presented in Eq. (12.5) is not flexible enough, therefore Polyansky *et al.* [41] used a multi-valued many body expansion [58] leading to a less accurate fit than we aspired to.

The BO-surface, constructed from 69 points of the Gaussian Geminals Ansatz combined with about additional 130 points from CI-R12 calculations (CIR12f) [41], which represents the electronic energy part (the *ab initio* data are already published in Refs. [28, 41]), has been 'corrected' by adding the diagonal adiabatic contributions, calculated on the FULL-CI level [32]) (see Section 2.3). The rms-errors of the fit of the BO part for the combination of GG with CIR12f, and of GG with CIR12d are similar: ≈ 0.35 cm^{-1} for a fit of 16th degree with 202 points. In the present work only results from the combination GG with CIR12f (GGCIR12f) are given, because the deviations of CIR12f, for the 69 GG points, is at most 0.5 cm^{-1} (as stated in [41]), whereas in case of CIR12d the deviation was much larger, 4.3 cm^{-1}. Within the combined data fit GGCIR12f the highest energy point lies at ≈ 70000 cm^{-1}; the data points include R_{H-H_2} distances up to 8 a$_o$. A plot of the potential is shown in Fig. 12.3. The result of our fit is a close reproduction of the GG-quality in the minimum region (up to ≈ 20000 cm^{-1}) and beyond that region the polynomial expansion basically represents CI-R12f-quality.

The difference between the potentials GG and CIR12f is presented in Fig. 3a of Ref. [30], and shows deviations smaller than 1 cm^{-1} for the range of $r(H_2)$: 0.8 to 2.5 a$_o$ and R(H-H$_2$): 1.0 to 3.0 a$_o$. Similar investigations for CIR12f and CIR12d show larger deviations (for details see [30]).

2.1.4 Results of the fit with full CI. In order to test in more detail the different functional forms for the fit, we calculated with DALTON [68] on full CI level (here called FCI, using the $(7s3p1d)/[5s3p1d]$ basis set of Augspurger and Dykstra [69] and the $(10s4p2d)/[7s4p2d]$ basis set of Meyer *et al.* [16]) electronic energies for several excited states (singlet and triplet states) using different coordinates with different distributions of data points. For the electronic ground state ($^1A_1$) differ-

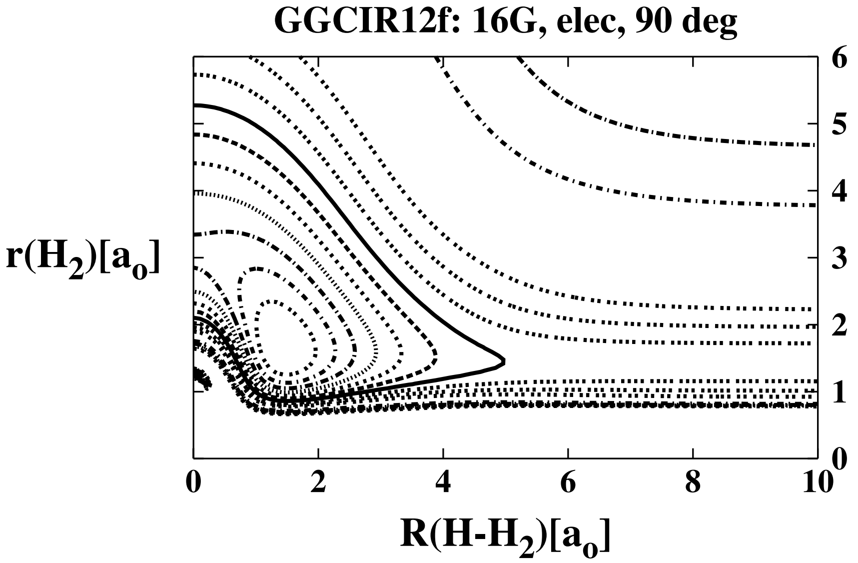

Figure 12.3. Extended **BO** potential energy surface of H_3^+ for GGCIR12f (innermost contour at 5000 cm^{-1}, next contours in steps of 5000 cm^{-1}). The coefficients of the fit are given in [30].

ences between results using GG, CI-R12 and FCI (with different basis sets) are shown in Fig. 12.4.

Preliminary results of the different fits (using a polynomial expansion and the reproducing kernel Hilbert space method) are discussed in the following and in the next Section. Vibrational eigenvalues, calculated with these FCI-potential fits, are discussed in Section 4.1 and presented in Table 12.1.

Fitting of ground and excited states becomes difficult if for all fits the same accuracy is needed. The form of the potential for the different electronic states looks completely different, and so one needs to use more flexible fit-functions.

Because the results also depend on the chosen grid of conformations, *ab initio* calculations (using the smaller $(7s3p1d)/[5s3p1d]$ basis set) have been performed for several grids (equidistant grid in Jacobi coordinates, the MSADC-grid (see Eqs. (12.1-12.4)), equidistant x, y, z-grid (see Eqs. (12.16))). For more than 10000 conformations 10 - 20 electronic states

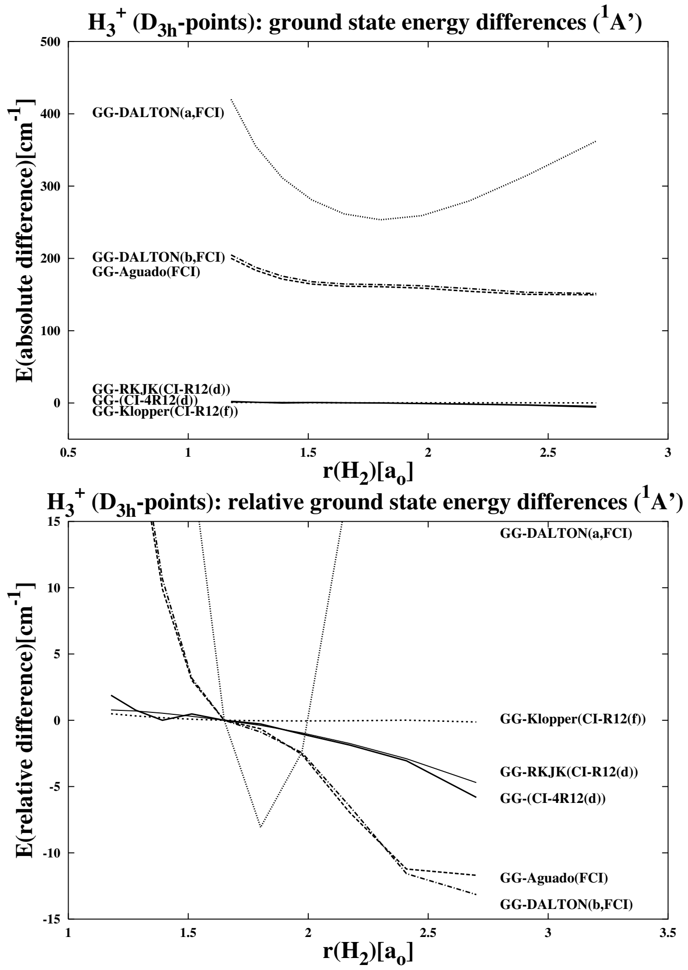

Figure 12.4. D_{3h}-symmetry: (top) Absolute energy differences between Gaussian Geminals (GG) and other methods and (bottom) relative energy differences (reference point: minimum at $r(H_2)=1.65a_0$) between GG and other methods. (GG: Gaussian Geminals [27]; RKJK: CIR12d [17]; CI-4R12(d): CIR12d with r_{12}-terms for the first four Slater determinants [66]; Klopper: CIR12f [41]; Aguado(FCI): full CI [43]; DALTON(a,FCI): full CI with $(7s3p1d)/[5s3p1d]$ basis, this work; DALTON(b,FCI): full CI with $(10s4p2d)/[7s4p2d]$ basis, this work).

Table 12.1. H_3^+: Comparison of vibrational eigenvalues ν_1, ν_2^l (J=0: even and odd states; TRIATOM code) calculated with potentials based on Gaussian Geminals (GG) (only electronic contributions) and other conventional *ab initio* methods (full CI (FCI)). Comparison of potentials based on polynomial (poly) expansions and the RKHS method. (Energies in cm^{-1}; mass: NU23).

		E_{ref}^{NU23}	$E(\Delta(E - E_{ref}^{NU23}))$					
	ν_1, ν_2, l	GG	MBB[a]	A[b]	FCI[c]	FCI[d]	FCI[e]	FCI[f]
		69(10)[g]	69(7)	69(7)	69(10)	69	335	335
			MBB[h]	'MBB'	AD	AD	AD	MBB
		poly	poly	poly	poly	RKHS	RKHS	RKHS
even	011	2521.08	-2.14	-2.13	-0.18	-0.11	-2.67	-6.60
	100	3179.04	-0.57	-0.87	7.37	7.57	6.47	-1.86
	020	4777.55	-4.86	-4.88	-0.38	-0.06	-19.83	-31.72
	022	4997.48	-4.60	-4.66	0.07	0.39	0.55	-4.21
	111	5554.58	-3.05	-3.35	7.24	7.42	7.40	-4.64
	200	6263.50	-1.36	-1.73	15.01	15.28	13.69	-3.16
	031	7005.03	-7.83	-7.89	-0.51	0.19	-21.21	-33.59
	033	7284.51	-8.58	-8.54	-0.02	0.57	-13.19	-21.90
	120	7769.25	-4.17	-4.74	7.41	7.56	8.92	-6.39
	122	7870.03	-5.81	-6.13	7.20	7.43	6.82	-7.17
	211	8488.71	-4.03	-4.40	14.74	14.81	17.91	-2.99
	040	9000.01	-11.36	-11.42	-1.51	-0.71	-25.22	-39.50
	042	9111.38	-11.95	-11.88	-1.84	-0.99	-21.18	-33.15
	300	9253.79	-2.20	-2.56	22.73	22.79	21.93	-4.32
	131	9652.82	-9.82	-9.94	2.69	3.51	-6.53	-21.52
	133	9967.40	-9.90	-10.25	5.58	5.74	-14.52	-29.78
	044	9996.79	-6.84	-7.48	6.75	7.21	11.88	-1.46
	220	10593.23	-5.44	-5.95	15.28	15.17	22.45	-2.92
odd	011	2521.08	-2.14	-2.13	-0.18	-0.04	-2.86	-6.73
	022	4997.48	-4.60	-4.66	0.07	0.44	-0.49	-4.48
	111	5554.57	-3.05	-3.35	7.24	7.44	7.28	-4.17
	031	7005.03	-7.83	-7.89	-0.51	0.14	-21.18	-33.76
	033	7492.54	-6.54	-6.68	1.09	1.69	12.42	7.21
	122	7870.03	-5.81	-6.13	7.20	7.42	6.31	-7.19
	211	8488.70	-4.03	-4.40	14.74	14.82	17.91	-2.29
	042	9111.33	-11.95	-11.88	-1.85	-0.99	-21.93	-33.03
	131	9652.81	-9.82	-9.94	2.69	3.56	-6.61	-21.15
	044	9996.78	-6.84	-7.48	6.75	7.17	12.46	-1.25
	133	10209.58	-7.79	-8.01	8.49	8.79	21.91	5.89

[a]: this work: original MBB points (Table III in [16]), 7th order polynomial fit; [b]: this work: original points from Aguado *et al.* [43] (given as EPAPS Document, Ref. 30 in [43]); basis set comparable wit MBB; 7th order polynomial fit. Similar results for 2400 points (given in the EPAPS Document [43]; 10th order fit) up to 23250.70 cm^{-1}; [c]: this work: Augspurger-Dykstra basis [69]; [d]: this work: Augspurger-Dykstra basis [69]; original 69 points, β=1., rms-error: 0.8 cm^{-1}; [e]: this work: Augspurger-Dykstra basis [69]; 335 points, xyz-grid, β=1., rms-error: 4.4 cm^{-1}; [f]: this work: MBB-basis [16]; 335 points, xyz-grid, β=1., rms-error: 5.5 cm^{-1}; [g]: number of data points (order of polynomial fit); [h]: basis sets.

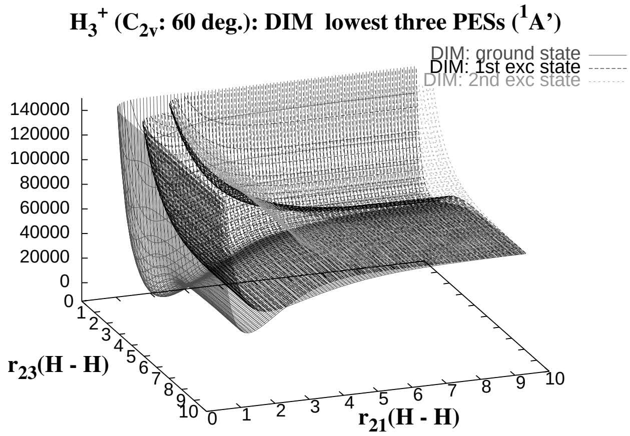

Figure 12.5. Plot of the three lowest electronic states of H_3^+ calculated with the 'diatomics-in-molecules'-method [48].

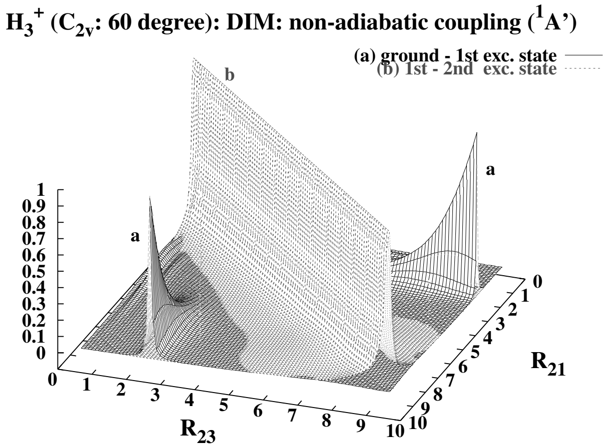

Figure 12.6. Plot of the first derivative coupling between the ground and first electronically excited state and as well the first and second electronically excited state of H_3^+ calculated with the 'diatomics-in-molecules'-method [48].

are available. We have to face for the PESs avoided crossings, real crossings (R= large, $r(H_2)$=2.5a_0), conical intersections (D_{3h}-symmetry: double degeneracy of 1st and 2nd excited state) and for the adiabatic and non-adiabatic couplings a complicated singular behavior at the energy crossings and conical intersections (see Figs. 12.5 and 12.6 as a demonstration of the whole complexity). A good place to start is to fit the original data to DIM-surfaces and to fit the residuum in a conventional way (similar work is done by Aguado *et al.* [43]). The results for excited states and the fitting of these data will be presented in a forthcoming paper; for the lowest states adiabatic and non-adiabatic couplings (first and second derivatives) have been calculated using the program package of Röhse [32] (see Section 2.3).

2.2 Fit with the reproducing kernel Hilbert space method

The reproducing kernel Hilbert space method (RKHS) is one of the new most promising methods, which can be used for fitting surfaces of polyatomic molecules. Ho and Rabitz [60] tested the method using the 69 CI-R12 points of Röhse *et al.* [17]. They got for different regularization schemes overall data residuals $\mathcal{R}(\alpha) \approx 0.4 - 0.5$ cm^{-1}. It was reported that (a) the RKHS-fit compares favorably with the fit of Röhse *et al.* [17] in the region where *ab initio* data are given, (b) the RKHS-surface is softer along the sides leading to the dissociation into H^+ + H_2 limit, and (c) the *a posteriori* error bound is essentially identical (within 1.0 cm^{-1}) to that of Röhse *et al.* Interestingly, it is found that in case of the RKHS-surface the error bound is small not only in the sampling region ($<$ 10 cm^{-1} for $r_{H-H} < 4a_0$), but also beyond it (10 - 300 cm^{-1} for $4a_0 < r_{H-H} < 7a_0$). We extended these investigation by using an improved set of data.

A Hilbert space of real-valued functions is called a reproducing kernel (r.k.) Hilbert space (RKHS) if all its evaluation functionals are continuous (Ho and Rabitz [60]). One assumes for the PES $V(\mathbf{R})$ as a bounded linear function the following reproducing property (with the reproducing kernel $Q(\mathbf{R},\mathbf{R}')$)

$$V(\mathbf{R}) =< Q(\mathbf{R},\mathbf{R}'), V(\mathbf{R}') >', \tag{12.10}$$

where the prime (') indicates that the inner product $<, >'$ is taken over the variable $\mathbf{R}'$. The reproducing property can be reformulated as a linear inverse problem with discrete data (*ab initio* points $\mathcal{V}(\mathbf{R}_\kappa), \kappa = 1, 2, .., M$) as

$$\mathcal{V}(\mathbf{R}_\kappa) =< Q(\mathbf{R}_\kappa,\mathbf{R}'), V(\mathbf{R}') >', \qquad \kappa = 1, 2, .., M, \tag{12.11}$$

where the goal is to invert this relation to find $V(\mathbf{R})$. The f-dimensional r.k. $Q(\mathbf{R},\mathbf{R}')$ can be constructed from the product relation

$$Q(\mathbf{R},\mathbf{R}') = \Pi_{i=1}^{f} q_i(x_i, x_i'), \tag{12.12}$$

where $q_i(x_i, x_i')$ is the r.k. associated with the one-dimensional RKHS having the reproducing property $g(x_i) =< q_i(x_i, x_i'), g(x_i') >'$ for each function $g(x_i)$. One looks for a regularized solution $V_\alpha^+(\mathbf{R})$, with a regularization parameter $\alpha > 0$, that minimizes the functional

$$\Phi(V;\alpha) = \parallel \mathbf{Q}V - \mathcal{V} \parallel^2 + \alpha \parallel V \parallel^2 . \tag{12.13}$$

The potential for H_3^+, $V(R_{12}, R_{23}, R_{31})$, is constructed from the 3D r.k. [60]

$$q^{m,n,k}(x,y,z,x',y',z') = q_2^m(x,x')q_2^n(y,y')q_2^k(z,z'), \quad 0 \le x,y,z \le 1, \tag{12.14}$$

where $q_2^m(x,x')$, $q_2^n(y,y')$, $q_2^k(z,z')$ are angle-like 1D r.k.s defined as

$$q_2^m(x,x') = \sum_{i=0}^{m-1} x_>^i x_<^i + m x_<^m x_>^{m-1} + {}_2F_1(1,-m+1;m+1;\frac{x_<}{x_>}). \tag{12.15}$$

x, y, z are the normalized basis defined as (with $\Gamma_1 = S_a$, $\Gamma_2 = S_e^2$ and $\Gamma_3 = S_e^3 \cos 3\phi$; see Eqs. (12.1-12.4))

$$x = [\Gamma_1 + \frac{\sqrt{3}}{\beta}(e^\beta - 1)]/[\frac{\sqrt{3}}{\beta}e^\beta], \quad y = \Gamma_2/[\frac{2}{3}(\frac{e^\beta}{\beta})^2] \tag{12.16}$$

$$z = [\Gamma_3 + (\sqrt{\frac{2}{3}}\frac{e^\beta}{\beta})^3]/[2(\sqrt{\frac{2}{3}}\frac{e^\beta}{\beta})^3] \tag{12.17}$$

In our first investigations [30] the RKHS-method was used for M=69 Gaussian Geminals *ab initio* data points. For m=12, n=6, k=3 and different regularization schemes (see [60]) similar overall data residuals $\mathcal{R}(\alpha) \approx 0.4 - 0.5$ cm^{-1} are obtained. The fit within the RKHS-method is performed with a set of data given which result from the original S_a, S_x, S_y distributions and are therefore clustered within the x, y, z distribution. For FCI *ab initio* data (DALTON) we compared additionally the fitting quality for regularly gridded distributions in S_a, S_x, S_y and x, y, z space.

One way of classifying the different fits is to compare the vibrational band origins. In Table 12.1 we show vibrational eigenvalues (and differences) which have been calculated with potentials based purely on the BO electronic contributions. We compare Gaussian Geminals (GG) (1st energy column) with FCI calculations (MBB and A are of FCI type) using polynomial and RKHS fits based on different representations of data points. We compare the fits for the original 69 and new 335 points based on Eqs. (12.1-12.4). Another way of classifying the quality of the fit is to present the surface in a plot with appropriate coordinates. Using

Jacobi coordinates one cannot clearly see that in case of homonuclear triatomic systems (like H_3^+) three identical arrangement channels have to result from the fit. On the other hand for hyperspherical coordinates this is possible: we compare a RKHS (Fig. 12.7a) with a polynomial fit (Fig. 12.7b). We can see lack of symmetry (RKHS-fit) resulting from not well chosen representation of coordinates within the fit-function (a subsequent symmetrization is needed). The plot is created by using a stereographic projection in hyperspherical coordinates ρ, θ, ϕ_τ (see Pack and Parker [71]) with the stereographic projection $X = \tan\left(\frac{\theta}{2}\right)\cos\phi_\tau$ and $Y = \tan\left(\frac{\theta}{2}\right)\sin\phi_\tau$. Within the ansatz of Pack and Parker six arrangement channels appear instead of the expected three because of inversion symmetry in the ϕ_τ coordinate. On the contrary, if an explicit expansion in symmetry adapted coordinates is used (polynomial fit: see Eqs. (12.1-12.4)) the symmetry is conserved (see Fig. 12.7b).

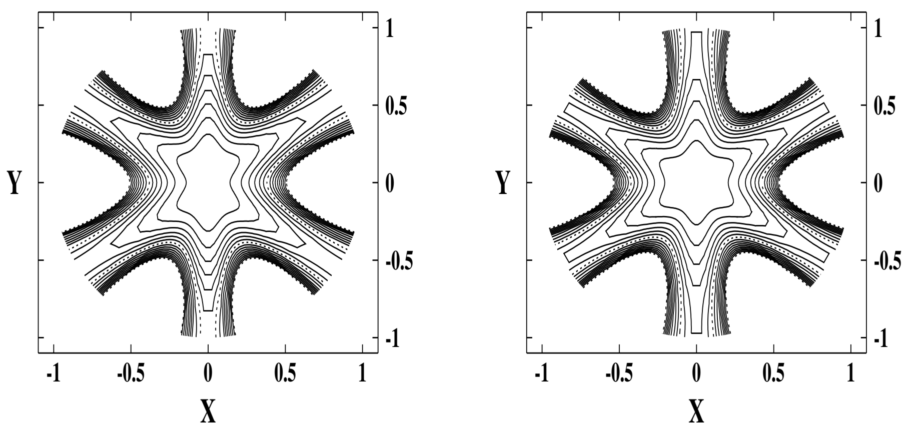

Figure 12.7. Potential energy contour map (full CI (FCI) calculated with DALTON [68]) of H_3^+. (a) (left) RKHS-fit method: 225 points (MBB-scheme) plus points in the asymptotic region. Stereographic projection $X = \tan\left(\frac{\theta}{2}\right)\cos\phi_\tau, Y = \tan\left(\frac{\theta}{2}\right)\sin\phi_\tau$: the hypersperical radius is fixed to $\rho = 2.1827a_0$. (b) (right) Polynomial fit method: 69 points (MBB-scheme). Stereographic projection: $\rho = 2.1827a_0$. Contours are given in steps of 5000 cm^{-1} starting from the interior region. The contour at 35000 cm^{-1} (not too far from the dissociation limit $H^+ + H_2$) is highlighted (dashed line).

2.3 Fit of adiabatic corrections

For a system containing only light nuclei the (diagonal) adiabatic correction is clearly the most important correction to the electronic PES.

To evaluate it we use the formula popularized by Handy [72–74]

$$E_{\mathrm{ad}} = -\sum_{Q_i} \frac{1}{2M_i} \int \Psi \frac{\partial^2}{\partial Q_i^2} \Psi \, d\tau, \tag{12.18}$$

which represents nothing but the expectation value of the kinetic energy of the nuclei (expressed in laboratory coordinates) computed with the electronic wave function Ψ. Q_i stands for a coordinate of the nucleus with the mass M_i and the integration goes over all the electronic coordinates. To arrive at this formula, Handy has used the ansatz of Born [75] for the total wave function, *i.e.* a single product of nuclear and electronic functions, *expressed in laboratory coordinates.* Since such functions are not normalisable, his derivation cannot be regarded as a rigorous justification of Eq. (12.18). This equation is pretty simple in contrast to the earlier extremely cumbersome expressions involving internal coordinates specified after separating the center-of-mass motion (COM) [76]. It has been shown by Kutzelnigg [77] that Eq. (12.18) is correct and can also be derived from a rigorous treatment starting with the separation of COM. Much earlier derivations of this formula go back to the work on diatomic molecules of Watson [78, 79] and Herman and Asgharian [80], where Watson (1973) also indicates that this form is more convenient for evaluation in *ab initio* calculations and that a generalization to polyatomic molecules is obvious.

Since the adiabatic contributions do not look like a Morse-type potential, but behave more like a smooth, flat surface in the range of the given geometrical points, a power series expansion in SADC (see Eqs. (12.1-12.3)) of 7th order gives nearly the same variance of 0.008 cm^{-1} (this includes the mass pre-factor) as a fit in MSADC of 9th order.

The fit for the adiabatic correction is performed for a symmetrical $\tilde{V}_s^{adia}$ and asymmetrical part $\tilde{V}_a^{adia}$ [21] (for the l^{th} isotopomer):

$$V_s^{adia} = \frac{1}{\mu_s^l} \tilde{V}_s^{adia} = \Big(\sum_i^3 \frac{1}{M_i}\Big) \frac{(\sum_i^3 f_i(\underline{Q}))}{3}, \quad f_i(\underline{Q}) = -\frac{1}{2}(\Psi|\Delta_i|\Psi) \tag{12.19}$$

$$V_a^{adia} = \frac{1}{\mu_a^l} \tilde{V}_a^{adia} = \Big(\frac{1}{M} - \frac{1}{m}\Big) \frac{1}{3}(2f_1 - f_2 - f_3). \tag{12.20}$$

with the electronic wave function Ψ and the expectation value of the kinetic energy with respect to the nuclear motion $\underline{Q}$ of nuclei i. M and m are different masses as given in H_2D^+ ($M{=}M_{\mathrm{D}}$, $m{=}M_{\mathrm{H}}$) or D_2H^+ ($M{=}M_{\mathrm{H}}$, $m{=}M_{\mathrm{D}}$). For symmetric mass combinations (*i.e.* H_3^+, D_3^+) the asymmetrical adiabatic contribution is zero (for further details: see Jaquet *et al.* [28, 30]).

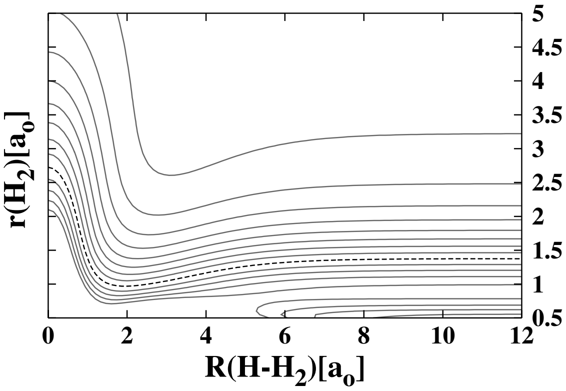

Figure 12.8. Absolute values of the diagonal adiabatic corrections (GG) for the electronic ground state (Jacobi coordinates, 90 degree): Extension of the plot into the asymptotic region. The fit for the adiabatic corrections results from *ab initio* points given in the inner region (69 points, 7th order fit, β=1.). Contour values (starting with 95 cm^{-1} in the inmost region) increase in steps of 5 cm^{-1} . The dashed contour at 115 cm^{-1} goes through the energy minimum.

Recently, new calculations have been performed to calculate adiabatic and non-adiabatic corrections on FULL-CI [32] level for different electronic states [30]. For the ground state we fitted the diagonal adiabatic corrections at about 200 positions on the surface for which GG or CIR12f points were available. The quality of the FULL-CI calculations compared to the GG-method is such that at the potential minimum the results of Cencek *et al.* [27] of V_s^{adia}=115.139 cm^{-1} deviate by 0.16 cm^{-1} from our new results (115.31 cm^{-1}). The difference between the polynomial fit of GG (69 points for the minimum region) and FULL-CI (200 points for an extended region) data can be seen by comparing Fig. 12.8 and the inner region of Fig. 12.9a; three different angles are presented in Fig. 12.9.

3. Spectroscopy: Calculation of rovibrational energy levels

Perturbation theory is not reliable for the calculation of vibrational and rotational problems of floppy molecules, e.g. H_3^+. Variational methods have to be used, although compared to perturbation theory can become computationally costly. In the case of H_3^+ there have been many contributions in the literature to calculate the rovibrational energies and transitions variationally using basis set or grid-based methods with prob-

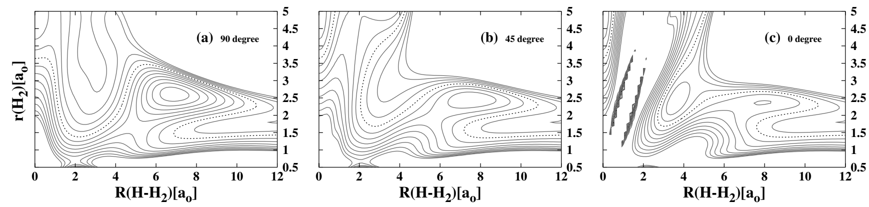

Figure 12.9. Diagonal adiabatic corrections for H_3^+, calculated from a FULL-CI wavefunction [32], given in Jacobi coordinates for three different angles. The fit is based on *ab initio* points spread over the whole area. Contours are given in steps of 5 cm^{-1}. The contour at 115 cm^{-1} going through the minimum of the PES is emphasized. The region around $r = 2.5a_0$ for $R > 8a_0$ is not correctly described, because for the polynomial fit the singular type of coupling (as indicated in Fig. 12.6) at $r = 2.5a_0$ has been excluded. The coefficients of the fit are given in [30].

lem adapted coordinates (for further discussion on rotation-vibration states, see Tennyson [81]).

We have performed quantum mechanical variational calculations for the rovibrational states of H_3^+ and all their isotopomers, using (a) the method of Sutcliffe and Tennyson [82,83] for triatomic molecules, implemented in the program packages TRIATOM [84] and DVR3DRJ [105] and (b) our own finite element (FE) program package FEMEIG [85] for up to three degrees of freedom. Within the FE-method (using different FE-grids) we solve a set of two-dimensional problems for the Jacobi-coordinates R and r, and then the angular part is solved with a DVR-method using associated Legendre function based grid points. The total wavefunction results from a diagonalisation of the Hamiltonian expanded in a product basis of FE and DVR grid points [86–88].

3.1 General aspects

In TRIATOM the quantum mechanical calculations of the rovibrational states [84] are based on Jacobi type scattering coordinates R(H-H_2), $r(H_2)$ and $\theta(R,r)$. Products of one-dimensional Morse oscillator functions for the R and r coordinates and associated Legendre polynomials $\Theta_{j,k}(\theta)$ (where j represents the rotation of the H_2^+ or H_2 and k is the projection of the total angular momentum J on the body-fixed z-axis) are used. The optimal parameters for the Morse functions are described in [28,89]. TRIATOM is not adapted to the full D_{3h} symmetry of H_3^+ but only to C_{2v}, so that for this system basis functions with even angular components (j even) are treated separately from those with odd ones (j odd). For the modes of H_3^+ belonging to E symmetry, one component of degenerate pairs of eigenvalues should be found with j even and one with j odd. Exact degeneracy between these pairs obtained independently, can be regarded as a test of convergence.

Rotationally excited levels ($J > 0$) were obtained by using a two-step variational procedure. In the first step, an intermediate basis set is generated, ignoring the effects of Coriolis coupling. In this step k (signed), the projection of the angular momentum J onto the molecule-fixed z-axis (embedded along R), is assumed to be a good quantum number and for each J, k-block ($k = 0$ to J) 1700 basis functions selected on an energy ordering criterion were used, and the lowest 600 non-Coriolis coupled eigenfunctions were computed. In the second step the off-diagonal coupling (k to $k \pm 1$) is included. The full secular matrix diagonalized in this step consisted of $(J + 1) \times 600$ basis functions derived from the first step calculation. In order to achieve higher accuracy for higher eigenstates we extended the calculations to a selection from 3000 basis functions and used $(J + 1) \times 800$ basis functions for the secular matrix. One has to keep in mind that there is also a vibrational angular momentum quantum number l that can range from n to 1 or 0 in steps of 2 if the degenerate vibrational mode ν_2 is n fold excited. Neither l nor k are rigorous quantum numbers; states can be classified by the approximate quantum number $G = |k - l|$.

The selection rules for the transitions are as follows. For H_3^+ with three spin (1/2) nuclei one state with total spin $I = 3/2$ (ortho H_3^+) and two states with spin $I = 1/2$ (para H_3^+) are possible. The nuclear spin wave function of ortho H_3^+ is totally symmetric with respect to exchange of the particles, while that of para-H_3^+ is partially antisymmetric. If one ignores the very small hyperfine interaction three quantum numbers can be regarded as good quantum numbers: the total angular momentum J, the parity $\pm$ and the total nuclear spin angular momentum I. Rigorous selection rules are $\Delta J = 0$ or ± 1, $+ \leftrightarrow -$ and $\Delta I = 0$ for single photon electric dipole transitions. The last selection rule can be interpreted in the sense that ortho ($G = 3n$) to para ($G = 3n \pm 1$) transitions are forbidden (n integer). The parity change is related to $\Delta k = \pm 1$ (with parity $= (-1)^k$). Because of symmetry restrictions some eigenstates do not exist: most notably the vibrationless states for J even and $G = 0$. The physical ground state of para-H_3^+ is ($J = 1, K = 1$) (with $K = |k|$), but for ortho-H_3^+ ($J = 1, K = 0$) [8]. For further details about symmetry, selection rules, assignments and forbidden rotational transitions, see Quack [90], Watson [8], Lindsay and McCall [51], and McCall [52].

3.2 Mass considerations, adiabatic and non-adiabatic effects

For the calculation of the nuclear dynamics there are several possible choices of mass (*i.e.* nuclear or atomic masses). Depending on the level of theory (see [27] and [28]), *i.e.* **BO** - approximation, BO plus adiabatic contributions, *etc.*, there are various possibilities to choose an appropriate mass for the simulation of experiment or for the deviations to complete theory [17, 77, 91, 92]: **NU**=1.0072764 a.m.u. for the nuclear masses, **AT**=1.007825035 a.m.u. for atomic (nuclear plus electronic) masses, **RE** for rescaled masses and **NU23**=1.0076421 a.m.u. for nuclear masses, each nucleus augmented by two-thirds of an electron mass considering heuristically in this way that there is a total of three nuclei and two electrons. In our case **NU23** can be also considered as an atomic mass. The four different masses (**NU, AT, RE, NU23**) have their own justification [28]. We have shown [29] that the influence of non-adiabaticity can be simulated by taking into account that the vibrational and rotational motion are related to different effective masses. Bunker and Moss [92] showed that special masses can be used for the vibrational motion and rotational motion to simulate non-adiabatic effects. The analysis of H_2 has shown that adiabatic and non-adiabatic contributions to the first three frequencies are of the size of 2.2 - 5.8 cm^{-1}, and that adiabatic corrections are of the same order of magnitude as non-adiabatic corrections. This means that if one is interested in high accuracy for spectroscopic properties or reaction dynamics the concept of a potential energy surface is not justified anymore; in our calculations for the rovibrational spectrum of H_3^+ we have reached this point.

NU23 mass is a fairly good choice for simulating non-adiabatic corrections, especially when low vibrationally excited states are involved [27, 28]. The errors for the **NU** mass at low transition frequencies or absolute energies for term values give a hint of the magnitude of the non-adiabatic contributions to different vibrationally excited states. Because the error for the term values starts with ≈ 0.0 cm^{-1} within a rotational series one might assume that for low vibrationally excited states the mass for the vibrational motion is well chosen, but for the rotation a modified mass (smaller than **NU23**) has to be taken. This is in agreement with the work of Bunker and Moss [92] on H_2 and Moss [91] on H_2^+ and its isotopomers. These authors propose to use for a hydrogenic system a vibrational reduced mass with a factor of ≈ 1.001 larger than the nuclear reduced mass and a rotational reduced mass with a factor of ≈ 1.0005 larger than the nuclear reduced mass. This means that in the case of H_3^+ appropriate masses would be the 'atomic mass' **NU23** for vibration and 'nuclear mass' **NU** for rotation; this mass choice is only useful, if adiabatic corrections have been taken into account and non-adiabatic contributions have to be simulated.

In order to include the effect of different masses for vibration and rotation the following changes in the kinetic energy expressions have been performed: (a) atomic masses are used in the kinetic energy expressions for the R and r motion and (b) nuclear masses are used in the kinetic energy expressions for the θ motion and wherever angular momentum operators in the Hamiltonian occur. Because the θ motion describes some kind of internal rotation we think that this might be a reasonable choice in the present work. This procedure is identified by **NUVR**. On the other hand, one can choose also atomic masses for the θ motion and use nuclear masses only for the total angular momentum and its projections. The latter approach was used by Polyansky and Tennyson (PT) [31] (nuclear mass for rotational and an effective vibrational mass (**NU**-Moss) for vibrational motion) for H_3^+, H_2D^+ and D_2H^+. PT found that that the kinetic energy expression has to be modified by an additional term if vibrational and rotational masses are not the same. This extra term is not large, but was found to be important especially for H_2D^+ making the residues compared to experimental values systematically small and smooth. In case of H_3^+ this additional term seems to be not very important and was neglected in our approach. In an earlier work [29] we tested the quality of the "optimal vibrational mass" (**NU**-Moss = 1.0075372 a.m.u.) - as proposed in the work of Moss [91] for the H_2^+ molecule - for the R, r and θ motion H_3^+.

Table 12.2. Influence on the accuracy of the rovibrational spectrum: size of the contributions E to the potential and remaining errors of transition frequencies $\Delta\nu$ (in cm^{-1}).

various contributions	$\Delta\nu$	E
BO electronic potential energy surface	< 0.01	≈ 40000
Diagonal adiabatic corrections	< 0.01	≈ 115
Relativistic contributions (Breit-Pauli)	< 0.01	≈ -2.6
Nonadiab. corrections (1st and 2nd derivat.)	≈ 0.5	$\approx \pm 50$
Potential fit (global, local)	$\approx 1. - 0.05$	
QED Lamb-shift	0^a	≈ 0.27

a: Not known, assumed to be negligible.

Table 12.2 summarizes the factors that influence the accuracy of the rovibrational spectrum [27,28]. The largest error represents the fit of the potential energy and is for an 10th oder polynomial fit of the magnitude $\Delta E \approx 0.05$ cm^{-1}. Explicit non-adiabatic corrections are still missing, and are simulated by using different masses. Fitting the non-adiabatic corrections will be demanding. Additionally, the coupling to the electronically bound triplet state has not been taken into account, but is assumed to be small.

3.3 Applications

In recent years several groups have analyzed rovibrational eigenstates for H_3^+ and its different isotopomers. Vibrational term values up to the dissociation limit were calculated, and high rotationally excited states ($J > 20$) in the low energy regime (< 15000 cm^{-1}) had been investigated. Most of these calculations were based on less accurate PESs. The highly accurate CI-R12 and GG PESs (including adiabatic and relativistic effects) for H_3^+, H_2D^+, D_2H^+, and D_3^+ have been used by the groups of Jaquet *et al.* [17,18,28–30], Tennyson *et al.* [22,31,93], and Alijah *et al.* [94–98]. Mostly eigenvalues, not much higher then the barrier to linearity ($\approx$ 10000 cm^{-1} above zero point energy), had been calculated, because higher energy regions are based on much less dense ab initio points. In the most recent work of Schiffels *et al.* [98] (using our GG-PES [28]) band origins up to 13000 cm^{-1} have been investigated. In their work non-adiabatic effects have been modeled by empirical corrections, based on calculations using only the nuclear mass.

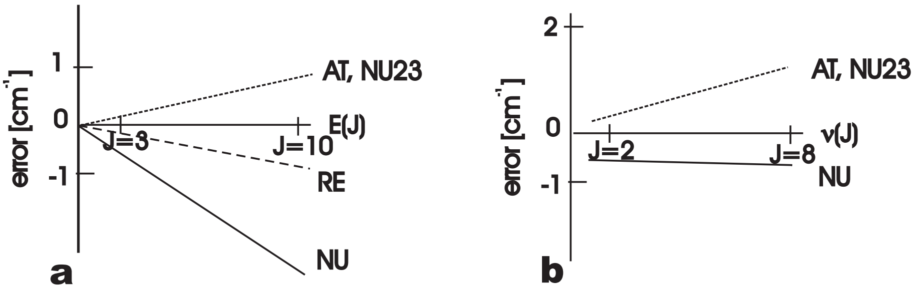

Figure 12.10. Sketch of the error-behavior (experim. - calc.[with adiabatic corrections]) for different masses depending on the total angular momentum J : (a) rovibrational eigenstates, and (b) rovibrational frequencies.

4. Calculation of transition frequencies

4.1 Transition frequencies below 7785 cm^{-1}

The calculated eigenstates and transitions for H_3^+, using adiabatic and relativistic corrections, showed a strong dependency on the choice of the mass for the nuclear motion [29]. In recent work we discussed the errors (comparing **NU** and **NU23**) for the term values $\nu_1\nu_2(l)$ and the bands $\nu_1\nu_2(l) \leftarrow \nu_1'\nu_2'(l')$ of H_3^+ for increasing energy ($\approx$ 1000 - 8000 cm^{-1}) or rotational quantum number J (ν_1 and ν_2 (double degenerate) are the vibrational modes with l as vibrational angular momentum quantum number). The results are summarized as a sketch in Fig. 12.10: atomic masses lead to small errors for low rotational quantum numbers (*i.e.* low energies) and the error increases linearly with total angular momentum J (deviations from experiment are $\epsilon \approx 0.$ - 1.4 cm^{-1}). For nuclear masses we could see roughly a constant deviation from the experimental result (*i.e.* a smaller variation in the error $\Delta\epsilon \approx 0.1$ - 0.3 cm^{-1}) which does not change very much with J. Larger deviations from the linear behavior of the error ϵ (for the term values and frequencies) indicate problems with proper assignment, because the deviations, although only a few tenths of a wavenumber, do not fit the overall behavior of ϵ. Similar analysis had been performed for H_2D^+ and D_2H^+ [29].

This mass behavior was the reason that lead us to the conclusion to test if the influence of non-adiabaticity can be simulated by using two different masses within one calculation. Similar considerations have been performed by Bunker and Moss [92] and Watson [78,79]. An overview of the lowest band origins of H_3^+ is given in Table 12.3 (see also Table 12.5) and term values and frequency bands are represented in Fig. 12.11. A comparison of the fundamentals of H_2D^+ and D_2H^+ together with D_3^+ is given in Table 12.4.

Analysis of the influence of the choice of masses on individual rovibrational states, including adiabatic corrections in the potential, shows the following:, (a) with nuclear masses the error reduces especially for the ν_1-mode or $\nu_1\nu_2$ combinations, (b) improvements of the ν_2 mode and its combinations $2\nu_2, 3\nu_2$ result from the small mass change, *i.e.* going from nuclear masses to atomic masses. In [29] we summarized all results by showing the deviations for all known term values and 12 bands with respect to experiment, where the influence of the choice of masses **NU, NU23**, the BO-approximation **BO**, diagonal adiabatic corrections **AD** and non-adiabatic simulations **NUVR** are presented. Although the adiabatic corrections to the electronic potential energy surface result in a nearly constant deviation of 0.5 - 0.7 cm^{-1} in the term values and of 0.1 - 0.3 cm^{-1} in the frequencies, the use of NUVR, *i.e.* simulating

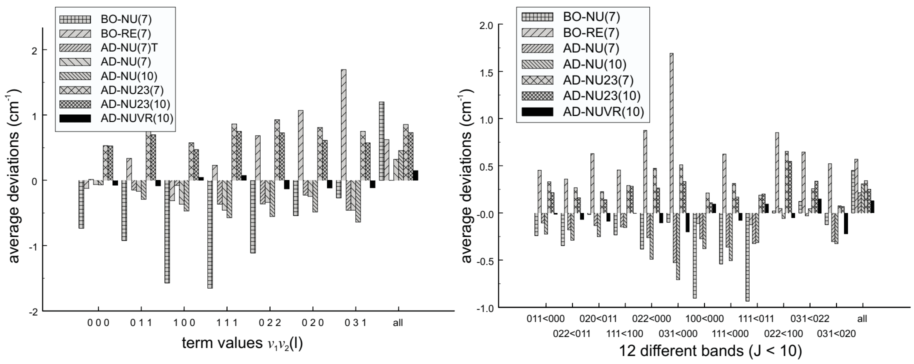

Figure 12.11. H_3^+: Term values and transition frequencies (in cm^{-1}). The deviation of the calculated values in comparison to experiment is given for different theoretical approaches (**BO**: Born-Oppenheimer, **AD**: with adiabatic corrections, masses: **NU, NU23, NUVR**). The number of input data for the histogram is given in [29].

Table 12.3. H_3^+: Comparison of band origins and vibrational term values ν_1, ν_2^l (in cm^{-1}), Different potentials and masses have been used.

$\nu_1\nu_2(l)$	RKJK[a] BO NU(7)	RKJK[a] BO RE(7)	JCRK[b] adia NU(10)	JCRK[b] adia NU23(10)	JCRK[c] non-adia NU-Moss(10)	JCRK[d] non-adia NUVR(10)	EXP[e]
ν_1	3179.35	3178.51	3178.68	3178.15	3178.301	3178.139	3178.29 (3178.16)[f]
ν_2^1	2521.59	2520.92	2521.62	2521.20	2521.322	2521.416	2521.409
$2\nu_2^2$	4998.40	4997.09	4998.53	4997.73	4997.956	4998.130	4997.965
$\nu_1\nu_2^1$	5555.49	5554.03	5554.85	5553.95	5554.208	5554.151	5554.063
$3\nu_2^3$	7493.86	7491.89	7493.82	7492.61	7492.956	7493.210	7492.913
$\nu_1 2\nu_2^2$	7871.70	7869.65	7871.05	7869.82		7870.206	7870.016

[a]: RKJK potential: Röhse, Kutzelnigg, Jaquet, Klopper (CISD-R12) [17], 7th order fit; [b]: JCRK potential: Jaquet, Cencek, Rychlewski, Kutzelnigg (Gaussian geminals), electronic energy, relativistic and adiabatic corrections [28], 10th order fit; [c]: JCRK potential [29], using the "optimal vibrational mass" proposed by Moss [91], 10th order fit; [d]: JCRK potential [29], using atomic masses for vibrational motion and nuclear masses for rotational motion, 10th order fit; [e]: EXP: Refs. [46,51,99]; [f]: EXP+FITA: Ref. [25].

non-adiabatic contributions, reduces dramatically the error to roughly a *few hundreds of a wavenumber*. This might be even better by using instead of the atomic mass NU23 the mass NU-Moss for the vibrational motion. A compilation of all data is presented in Fig. 12.12, where we show the most recent deviations between experimental and theoretical

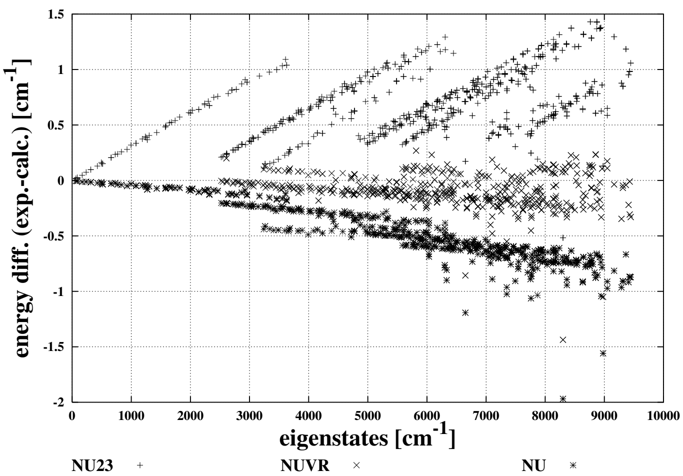

Figure 12.12. Rovibrational eigenstates differences (experim. [51] - calc.) (including possible misassignments in the literature) using different masses **NU23**, **NU**, and **NUVR**.

rovibrational eigenstates. A detailed picture is given in Fig. 3 of Lindsay and McCall [51], who compared their newest compilation of experimental data with the best theoretical results (using *ab initio* and semi-empirical potentials) available in the literature. We will discuss in the next Section details only for the frequency range of 7785 - 8164 cm^{-1}. Lindsay and McCall show that except for a small frequency range, Polyansky and Tennyson's [31] (using our CRJK-potential, based on GG) and our results [29] are in principle equivalent and scatter around zero deviation to experiment, when simulation of non-adiabatic effects is accounted for.

Table 12.5 shows higher band origins (A_1, A_2 and E states). Compared to mass NU23, mass NU leads to an increasing shift of the energies to higher values. The influence of using a potential, that is based on more *ab initio* points than before (GGCIR12f), is presented and for comparison the MBB-results are given. In the literature mostly theoretical rovibrational states have been published for that energy region (< 10000 cm^{-1}) for which experimental values had been available. For the original fit (GG, 69 points) a comparison of calculations with 1700 and 3000 basis functions (using TRIATOM) revealed that deviations start at ≈ 13000 cm^{-1} and increase to already ≈ 7.4 cm^{-1} at ≈ 16000 cm^{-1}. Although applications with the TRIATOM-code (see results in Table 4 in [30]) seemed to be stable, one could see that by using the DVR3DRJ program some smaller, increasing deviations occurred at en-

Table 12.4. Comparison of fundamentals of H_2D^+, D_2H^+ and D_3^+. Frequencies in cm^{-1}.

	RKJK[a] NU(7)	RKJK[a] RE(7)	RKJK+adia[b] NU(7)	JCRK[c] NU23(9)	EXP[d]
H_2D^+					
ν_1	2993.75	2993.16	2992.566	2992.377	2992.505
ν_2	2206.37	2205.93	2206.081	2205.944	2205.869
ν_3	2335.07	2334.60	2335.557	2335.411	2335.449
$(\nu_2+\nu_3)/2$	2270.72	2270.27	2270.819	2270.678	2270.659
$(\nu_3-\nu_2)$	128.70	128.67	129.476	129.467	129.580
D_2H^+					
ν_1	2737.84	2737.40	2737.011	2736.872	2736.981
ν_2	1967.65	1967.33	1968.262	1968.161	1968.169
ν_3	2079.44	2078.90	2078.623	2078.353	2078.430
$(\nu_2+\nu_3)/2$	2023.44	2023.12	2023.443	2023.257	2023.300
$(\nu_3-\nu_2)$	111.58	111.57	110.361	110.192	110.261
D_3^+					
ν_1	2301.40	2301.29		2301.029	
ν_2	1834.83	1834.73		1834.605	1834.67

[a]: RKJK-potential: BO-energies, 7th order fit [17]; [b]: RKJK+adia: RKJK-potential and SCF-level adiabatic corrections, 7th order fit [21]; [c]: this work: 9th order fit, including electronic energy, relativistic and adiabatic corrections; [d]: EXP: H_2D^+: [100, 101]; D_2H^+: [101, 102]; D_3^+: [103].

ergies below 13000 cm^{-1}. For the higher energy regime some eigenvalues are shifted down more strongly. Because of that reason new converged results have been presented in Table 12.5 using the DVR3DRJ code [105] with 8500 energy selected basis functions (spherical oscillator functions in the R-direction). These results have been confirmed by using the hyperspherical coordinate method [97] as applied by Alijah *et al.* [98].

The topic of small deviations between different programs using different coordinates has already been addressed in the work of Lindsay and McCall who compared the best theoretical data including hyperspherical coordinate applications. A comparison of Jaquet's and Alijah's rovibrational eigenvalues [104], using the same mass (**NU**) and assuming the same potential code, showed that there are significant differences with slight dependence on the vibrational state (see Fig. 4 in [51]). This problem has been clarified and results from slightly different fits (used by the authors of Ref. [98] and the present author) of the same ab initio data (i.e. fit of the total energy (electronic, adiabatic and relativistic contributions) compared to the sum of individual fits of the electronic, adiabatic and relativistic contributions). The deviations in the rovibrational eigenvalues (> 0.1 cm^{-1}) for the two different fits become obvious at higher energies (> 12000 cm^{-1}). We can confirm that there is no difference in the quality of the different fits with respect to the ab initio data: the deviations give a hint of the size of the theoretical error bar.

With the new potential GGCIR12f we find relatively large changes which tend to shift the eigenvalues mostly to higher values, although a few values, i.e. especially of A_2-symmetry, are shifted to lower energies. These unusual results have to be investigated further.

In Table 12.6 we present vibrational eigenvalues (and differences compared to GG results) which have been calculated for different potentials (FCI with various basis sets; polynomial fits) based just on the electronic contributions. In addition, we included the original work of Aguado *et al.* [43] and the the results which one gets if one refits the full CI data of Aguado *et al.* (as given in the EPAPS document, see Ref. 30 in [43]); the basis set of Aguado *et al.* is slightly better than the one of Meyer *et al.* [16]. We can see in Table 12.6 that MBB (2nd energy column) deviates from GG (1st energy column) by several wavenumbers. Eigenvalues resulting from refitting the Aguado *et al.* *ab initio* data (3rd energy column: fits with up to 2400 points – 23250.70 cm^{-1} above the minimum – have been used) are similar, as expected. On the other hand, Aguado *et al.* represent in their work a fit with which rovibrational eigenvalues and transition frequencies have been calculated. The difference of these results compared to our GG calculations (without relativistic and adiabatic corrections) is seen in the 5th energy column. The deviation is very small which one would not expect. This can only be explained by the fact that the fit in the work of Aguado *et al.* was performed for their full CI data under the constraints that the GG or CI-R12 data had to be nearly reproduced. This is documented in Table 12.7 which shows that the deviations, compared to GG and CI-R12, for three exemplary individual configuration points and the rms-error for the very 69 points with respect to the Aguado fit [43].

The rovibrational eigenvalues, using a potential based on the original data of MBB or on additionally extra calculated *ab initio* points (basis set: MBB), are comparable with those ones, which are calculated by us using the 'special' 69 points of the original *ab initio* data of Aguado *et al.* [43] (a plot of the potential energy differences is given in Fig. 12.4). The results for the Aguado *et al.* eigenvalues do not change if we fit

Table 12.5. H_3^+: Comparison of A_1, A_2 and E states[a] (ν_1, ν_2^l) calculated with the GG[b] and GGCIR12f[c] potential (in cm^{-1}). A large basis set (with 8500 basis functions) and different masses (**NU23, NUVR, NU**) have been used. Comparison with the MBB[d] results using atomic masses (**AT**).

	E_{ref}	$E(\Delta(E_{ref}))$		$E(\Delta(E_{GG,NU}))$	$E(\Delta(E_{ref}))$	
$\nu_1\nu_2^l$	GG	GGCIR12f	GG	GGCIR12f	GG	MBB
	NU23	NU23	NU	NU	NUVR	AT
	8500	8500	8500	8500	1700	8500
A_1						
100	3178.15	3178.17(0.02)	3178.68(0.53)	3178.70(0.02)	3178.14(-0.01)	(0.17)
020	4778.01	4777.86(-0.15)	4778.75(0.74)	4778.60(-0.15)	4778.39(0.38)	(-0.99)
200	6261.81	6261.89(0.08)	6262.84(1.03)	6262.92(0.08)	6261.79(-0.02)	(0.12)
033	7285.34	7286.79(1.45)	7286.43(1.09)	7287.89(1.46)	7285.85(0.51)	(-2.82)
120	7768.83	7769.68(0.85)	7770.06(1.23)	7770.91(0.85)	7769.25(0.42)	(0.26)
040	9001.39	9003.83(2.44)	9002.67(1.28)	9005.11(2.44)	9002.05(0.66)	(-4.66)
300	9251.41	9251.55(0.14)	9252.90(1.49)	9253.04(0.14)	9251.41(0.00)	(0.04)
133	9968.31	9970.35(2.04)	9969.76(1.45)	9971.80(2.04)	9968.84(0.53)	(-4.26)
220	10592.48	10594.18(1.70)	10594.11(1.63)	10595.81(1.70)	10592.89(0.41)	(-0.41)
053	10923.02	10931.66(8.64)	10924.42(1.40)	10933.06(8.64)	10924.14(1.12)	(-9.64)
140	11813.68	11817.74(4.06)	11815.38(1.70)	11819.44(4.06)	11814.81(1.13)	(-4.38)
400	12145.75	12146.02(0.27)	12147.67(1.92)	12147.94(0.27)		(-0.06)
060	12381.28	12399.98(18.70)	12382.65(1.37)	12401.36(18.71)		(-17.3)
233	12589.49	12594.56(5.07)	12591.26(1.77)	12596.33(5.07)		(-5.04)
320	13287.55	13291.43(3.88)	13289.48(1.93)	13293.37(3.89)		(-2.77)
	13403.92	13413.00(9.08)	13405.69(1.77)	13414.77(9.08)		(-11.9)
	13723.94	13747.42(23.48)	13725.52(1.58)	13749.00(23.48)		(-18.1)
	14196.41	14194.47(-1.94)	14198.35(1.94)	14196.41(-1.94)		(-10.4)
	14665.41	14669.40(3.99)	14667.59(2.18)	14671.58(3.99)		(-2.67)
	14906.38	14928.63(22.25)	14908.15(1.77)	14930.45(22.30)		(-20.0)
	14939.08	14940.82(1.74)	14941.36(2.28)	14943.07(1.71)		(-0.57)
	15077.94	15096.24(18.30)	15080.03(2.09)	15098.33(18.30)		(-16.4)
	15166.79	15181.91(15.12)	15168.85(2.06)	15183.96(15.11)		(-9.11)
	15875.18	15885.02(9.84)	15877.38(2.20)	15887.27(9.89)		(-7.55)
	15921.19	15938.95(17.76)	15923.34(2.15)	15941.09(17.75)		(-12.4)
	16215.60	16235.54(19.94)	16217.65(2.05)	16237.58(19.93)		(-20.6)
A_2						
033	7492.61	7490.23(-2.38)	7493.82(1.21)	7491.44(-2.38)	7493.21(0.60)	(0.03)
133	10209.65	10207.02(-2.63)	10211.23(1.58)	10208.60(-2.63)	10210.22(0.57)	(-1.11)
053	11529.14	11520.86(-8.28)	11530.85(1.71)	11522.57(-8.28)		(-3.39)
233	12830.44	12827.84(-2.60)	12832.35(1.91)	12829.75(-2.60)		(-2.02)
	13755.04	13749.53(-5.51)	13756.94(1.90)	13751.43(-5.51)		(-7.59)
	14565.47	14567.70(2.23)	14567.66(2.19)	14569.88(2.22)		(-1.64)
	15188.61	15190.04(1.43)	15190.68(2.07)	15192.11(1.43)		(-9.55)
	15370.77	15369.77(-1.00)	15372.99(2.22)	15372.00(-0.99)		(-2.86)
	15886.07	15887.94(1.87)	15888.31(2.24)	15890.18(1.87)		(-4.92)
	15964.71	15963.58(-1.13)	15966.79(2.08)	15965.68(-1.11)		(-12.8)
	16016.22	16025.55(9.33)	16018.39(2.17)	16027.72(9.33)		(-10.2)

Table 12.5: (Continued)

	E_{ref}	$E(\Delta(E_{ref}))$		$E(\Delta(E_{GG,NU}))$	$E(\Delta(E_{ref}))$	
$\nu_1\nu_2^l$	GG	GGCIR12f	GG	GGCIR12f	GG	MBB
	NU23	NU23	NU	NU	NUVR	AT
	8500	8500	8500	8500	1700	8500
E						
011	2521.20	2521.21(0.01)	2521.62(0.42)	2521.62(0.00)	2521.42(0.22)	(0.06)
022	4997.73	4997.74(0.01)	4998.53(0.80)	4998.54(0.01)	4998.13(0.40)	(-0.32)
111	5553.95	5554.05(0.10)	5554.85(0.90)	5554.94(0.09)	5554.15(0.20)	(-0.28)
031	7005.81	7005.83(0.02)	7006.86(1.05)	7006.88(0.02)	7006.34(0.53)	(-2.32)
122	7869.82	7869.97(0.15)	7871.05(1.23)	7871.19(0.14)	7870.21(0.39)	(-1.18)
211	8487.52	8487.70(0.18)	8488.86(1.34)	8489.04(0.18)	8487.72(0.20)	(-0.61)
042	9112.85	9114.97(2.12)	9114.14(1.29)	9116.25(2.11)	9113.51(0.66)	(-5.11)
131	9653.40	9650.33(-3.07)	9654.85(1.45)	9651.77(-3.08)	9654.04(0.64)	(-2.68)
044	9996.71	9997.98(1.27)	9998.27(1.56)	9999.54(1.27)	9997.36(0.65)	(-0.23)
222	10644.52	10644.90(0.38)	10646.13(1.61)	10646.52(0.39)	10644.94(0.42)	(-1.93)
051	10862.45	10871.14(8.69)	10863.86(1.41)	10872.56(8.70)	10863.51(1.06)	(-8.92)
311	11322.30	11322.71(0.41)	11324.05(1.75)	11324.45(0.40)	11322.54(0.24)	(-0.86)
055	11657.67	11657.63(-0.04)	11659.30(1.63)	11659.26(-0.04)	11658.98(1.31)	(-6.28)
142	12078.40	12078.16(-0.24)	12080.14(1.74)	12079.89(-0.25)		(-4.88)
231	12302.56	12306.92(4.36)	12304.21(1.65)	12308.61(4.40)		(-8.00)
144	12476.64	12490.29(13.65)	12478.27(1.63)	12491.90(13.63)		(-8.80)
062	12696.24	12700.32(4.08)	12698.13(1.89)	12702.22(4.09)		(-2.20)
322	13316.76	13318.34(1.58)	13318.71(1.95)	13320.29(1.58)		(-3.29)
	13394.31	13397.25(2.94)	13396.14(1.83)	13399.09(2.95)		(-8.77)
	13591.06	13595.32(4.26)	13592.86(1.80)	13597.12(4.26)		(-10.1)
	13701.08	13725.65(24.57)	13702.65(1.57)	13727.21(24.56)		(-19.6)
	14053.60	14054.67(1.07)	14055.70(2.10)	14056.77(1.07)		(-1.45)
	14216.48	14215.75(-0.73)	14218.50(2.02)	14217.78(-0.72)		(-5.28)
	14475.25	14480.59(5.34)	14477.19(1.94)	14482.53(5.34)		(-10.1)
	14888.15	14887.73(-0.42)	14890.33(2.18)	14889.91(-0.42)		(-9.61)
	14898.91	14919.89(20.98)	14900.74(1.83)	14921.72(20.98)		(-13.0)
	15120.76	15141.65(20.89)	15122.76(2.00)	15143.65(20.89)		(-17.2)
	15211.91	15217.30(5.39)	15213.99(2.08)	15219.37(5.38)		(-8.79)
	15333.88	15340.80(6.92)	15335.98(2.10)	15342.91(6.93)		(-8.83)
	15787.62	15786.15(-1.47)	15789.72(2.10)	15788.29(-1.43)		(-15.8)
	15886.07	15887.94(1.87)	15888.31(2.24)	15890.18(1.87)		(-4.92)
	16016.22	16025.55(9.33)	16018.39(2.17)	16027.72(9.33)		(-10.2)
	16261.58	16285.61(24.03)	16263.60(2.02)	16287.63(24.03)		(-18.2)

[a]: DVR3DRJ-code (8500 basis functions) [105] and TRIATOM-code (1700 basis functions; 5th energy column) calculations; [b]: GG-potential: 10th order fit, 69 points [28]; [c]: this work: GGCIR12f-potential; 16th order fit, 202 points; [d]: MBB-potential: 7th order fit, 69 points [16].

Table 12.6. H_3^+: Comparison of vibrational eigenvalues ν_1, ν_2^l (J=0: even and odd states; TRIATOM) calculated with potentials based on Gaussian Geminals (GG) (only electronic contributions) and conventional *ab initio* methods (full CI (FCI)). All potentials are based on polynomial (poly) expansions. (Energies in cm^{-1}; masses: NU23, NU).

	E_{ref}^{NU23}	$E(\Delta(E-E_{ref}^{NU23}))$				E_{ref}^{NU}	$E(\Delta(E-E_{ref}^{NU}))$		
$\nu_1\nu_2^l$	GG NU23	MBB[a]	A[b]	FCI[c]	A[d]	GG NU	MBB[a]	A[b]	FCI[c]
even	poly	poly	poly	poly	mbe	poly	poly	poly	poly
011	2521.08	-2.14	-2.13	-0.18	0.00	2518.41	0.94	0.96	2.90
100	3179.04	-0.57	-0.87	7.37	0.04	3185.51	-6.51	-6.80	1.43
020	4777.55	-4.86	-4.88	-0.38	0.06	4757.72	15.70	15.68	20.18
022	4997.48	-4.60	-4.66	0.07	0.05	4998.03	-4.35	-4.41	0.33
111	5554.58	-3.05	-3.35	7.24	0.01	5561.98	-9.56	-9.86	0.73
200	6263.50	-1.36	-1.73	15.01	0.07	6277.19	-14.03	-14.40	2.34
031	7005.03	-7.83	-7.89	-0.51	-0.06	6983.82	14.43	14.37	21.74
033	7284.51	-8.58	-8.54	-0.02	-0.03	7271.31	5.70	5.74	14.27
120	7769.25	-4.17	-4.74	7.41	0.02	7778.17	-11.85	-12.43	-0.28
122	7870.03	-5.81	-6.13	7.20	-0.01	7876.85	-11.40	-11.72	1.62
211	8488.71	-4.03	-4.40	14.74	0.16	8506.62	-20.60	-20.97	-1.83
040	9000.01	-11.36	-11.42	-1.51	-0.19	8974.80	15.13	15.07	24.98
042	9111.38	-11.95	-11.88	-1.84	-0.26	9090.19	10.51	10.59	20.62
300	9253.79	-2.20	-2.56	22.73	0.16	9275.72	-22.64	-22.99	2.29
131	9652.82	-9.82	-9.94	2.69	-0.28	9646.30	-1.84	-1.96	10.67
133	9967.40	-9.90	-10.25	5.58	0.44	9952.88	6.06	5.71	21.54
044	9996.79	-6.84	-7.48	6.75	0.16	10008.67	-17.15	-17.79	-3.56
220	10593.23	-5.44	-5.95	15.28	0.36	10615.67	-26.26	-26.77	-5.53
222	10644.88	-7.00	-7.36	13.91	0.48	10658.66	-19.17	-19.53	1.75
051	10860.58	-16.42	-16.30	-5.05	-0.96	10838.64	6.94	7.06	18.32
053	10920.66	-17.07	-16.83	-5.58	-0.60	10903.40	1.59	1.83	13.09
odd									
011	2521.08	-2.14	-2.13	-0.18	0.00	2518.22	1.13	1.15	3.09
022	4997.48	-4.60	-4.66	0.07	0.05	4996.99	-3.31	-3.36	1.37
111	5554.57	-3.05	-3.35	7.24	0.02	5561.85	-9.44	-9.74	0.85
031	7005.03	-7.83	-7.89	-0.51	-0.06	6983.85	14.40	14.34	21.71
033	7492.54	-6.54	-6.68	1.09	-0.10	7504.95	-17.74	-17.88	-10.11
122	7870.03	-5.81	-6.13	7.20	-0.01	7876.34	-10.89	-11.21	2.13
211	8488.70	-4.03	-4.40	14.74	0.17	8506.60	-20.60	-20.97	-1.82
042	9111.33	-11.95	-11.88	-1.85	-0.21	9089.40	11.25	11.33	21.36
131	9652.81	-9.82	-9.94	2.69	-0.27	9646.19	-1.76	-1.88	10.75
044	9996.78	-6.84	-7.48	6.75	0.16	10009.24	-17.73	-18.37	-4.15
133	10209.58	-7.79	-8.01	8.49	-0.05	10231.49	-28.12	-28.34	-11.83
222	10644.81	-7.01	-7.37	13.92	0.55	10657.86	-18.45	-18.81	2.49
051	10859.81	-16.46	-16.34	-5.06	-0.18	10836.26	8.49	8.60	19.89

[a]: original MBB points (Table III in [16]); this work: 7th order polynomial fit (69 points); [b]: original points from Aguado *et al.* [43] (given as EPAPS Document, Ref. 30 in [43]); this work: 7th order polynomial fit (69 points, MBB-grid). The results are very similar when using 2400 points (given in the EPAPS Document [43]; 10th order fit) up to 23250.70 cm^{-1}; [c]: Augspurger-Dykstra basis [69]; this work: 10th order polynomial fit (original 69 points); this work: RKHS-fit (original 69 points, β=1., rms-error: 0.8 cm^{-1}). this work: RKHS-fit (335 points, xyz-grid, β=1., rms-error: 4.4 cm^{-1}). [d]: Aguado *et al.*, from Table VI in [43], basis set comparable with MBB-basis, many body expansion (mbe) fit.

the potential with the 69 points as proposed by Meyer *et al.* or if we would include more points to get a better global potential. Taking all data of Aguado *et al.* even up to 35000-40000 cm^{-1} lead to minor changes for the vibrational eigenvalues.

Table 12.7. Deviations ΔE of the energy fit of Aguado *et al.* from the full CI data of Aguado *et al.* [43], the Gaussian Geminals (GG) energies of Cencek *et al.* (Table 1 in [27]) and the CI-R12 energies of Röhse *et al.* (Table 5 in [17]). The rms-error for the very 69 points suggested by Meyer *et al.* is presented; the minimum of the potential is at the position of the 5th point. (Energies in cm^{-1}).

	full CI	GG	CI-R12
	Aguado *et al.* [43]	Cencek *et al.* [27]	Röhse *et al.* [17]
rms (69 p.)	16.64	0.99	1.42
ΔE			
1st point	34.77	-3.07	-2.28
5th point	-0.78	-0.78	-0.78
69th point	-26.52	-1.40	-0.17

As already said, the results in Table 12.6 in the 2nd (MBB) and in the 3rd column (Aguado) are similar. Rovibrational eigenvalues based on FCI with a smaller basis set (Augspurger-Dykstra (AD) [69]) show larger deviations (4th column) compared to the improved basis sets. Table 12.1 shows small changes (69 points fit), if instead of the polynomial fit (4th column) a RKHS-fit (5th column) was used. If more *ab initio* points (335 point instead of 69) are included in the fit one can get within the RKHS method (AD-basis: 6th column; MBB-basis: 7th column) a reasonable rms-error of 4 - 5 cm^{-1}; in that case the vibrational eigenvalues are far off from what one gets if the points are more closely chosen to the minimum region. The 335 points are chosen from an equal distribution of grid points within the x, y, z-space fulfilling the triangle inequality condition (see Eq. (12.16)). If we would have chosen the same number of data points using the prescription of MBB [16], the points would have been clustered in the x, y, z-representation for the RKHS method leading to strong linear dependencies. This shows that although the potential energy surface (coming from the RKHS fit) is very smooth the resulting vibrational eigenvalues are off by several wavenumbers.

Table 12.8. Comparison of different theoretical results and the experimental data of McCall and Oka [50] for rovibrational transitions of H_3^+ near 1.25 μm (28 lines assigned to $\nu_1 + 2\nu_2^2 \leftarrow 0$ and 2 lines assigned to $2\nu_1 + \nu_2^1 \leftarrow 0$ (see $P(6,6), P(5,5)$) (frequencies in cm^{-1}). (Table adapted from [50]).

transition[a]	observed (cm^{-1}) McCall Oka	(observed - calculated)[b] adjusted potentials				*ab initio* potentials			
		Wat	NMT	Da	WH	Db	J[c] adiab new	J[d] adiab	J[d] non-ad
$^tQ(3,0)$	7785.233	-0.032	-0.297	-0.295	-0.347	-0.714	0.457	0.507	0.138
$^tQ(1,0)$	7785.701	0.361	-0.309	-0.307	-0.326	-0.721	0.463	0.490	0.122
$^tR(3,3)$	7789.878	-0.147	-0.282	-0.233		-0.715	0.535	0.495	0.085
$^nP(1,1)$	7805.893	0.043	-0.647	-0.645	-0.465	-1.038	0.126	0.175	-0.221
$^nP(2,2)$	7820.239	0.259	-0.351	-0.356	0.043	-0.738	0.408	0.488	0.116
$^tR(2,2)$	7822.375	0.125	-0.265	-0.251		-0.708	0.537	0.513	0.105
$^nP(3,3)$	7826.739	0.060	-0.381	-0.377	0.269	-0.741	0.376	0.494	0.160
$^nP(4,4)^l$	7833.249	-0.195	-0.421	-0.421	0.293	-0.745	0.356	0.497	0.189
$^tR(1,1)$	7850.959	0.283	-0.291	-0.284		-0.719	0.515	0.510	0.103
$^tR(4,3)$	7880.921	-0.522	-0.259	-0.214		-0.711	0.562	0.535	0.092
$^nQ(1,1)$	7894.711	0.333	-0.339	-0.335	-0.186	-0.737	0.465	0.510	0.154
$^nQ(2,1)$	7898.371	0.183	-0.329	-0.329	-0.266	-0.735	0.472	0.511	0.079
$^nQ(3,1)$	7905.717	-0.174	-0.313	-0.310	-0.378	-0.725	0.503	0.531	0.172
$^tR(3,2)$	7912.047	-0.148	-0.243	-0.242		-0.714	0.558	0.541	0.099
$^tR(2,1)$	7939.619	0.120	-0.271	-0.268		-0.713	0.548	0.547	0.135
$^tR(1,0)$	7970.413	0.288	-0.287	-0.285	-0.455	-0.717	0.553	0.549	0.112
$^nQ(2,2)$	7998.890	0.136	-0.350	-0.346	-0.050	-0.729	0.485	0.552	0.198
$^tR(4,2)$	8005.582	-0.858	-0.248				0.601	0.581	0.105
$^nQ(3,2)^u$	8007.410	-0.218	-0.350	-0.344	-0.260	-0.729	0.507	0.559	0.020
$^nQ(4,2)^u$	8022.012	-0.681	-0.318	-0.318	-0.426	-0.694	0.575	0.605	0.343
$^tR(3,1)$	8027.840	-0.497	-0.250	-0.244	-0.812	-0.698	0.594	0.602	0.015
$^nR(3,1)^l$	8037.673	-0.518	-0.337	-0.335		-0.754	0.499	0.551	0.153
$P(6,6)$	8053.382	-1.428	-0.528				0.354	0.331	0.207
$^nR(1,1)$	8071.617	0.203	-0.313	-0.316	-0.247	-0.720	0.542	0.579	0.085
$^nQ(4,3)$	8089.406	-0.876	-0.344	-0.344	0.034	-0.724	0.501	0.596	0.168
$^nQ(3,3)$	8110.069	-0.133	-0.381	-0.384	-0.079	-0.725	0.526	0.596	0.144
$P(5,5)$	8123.128	-0.857	-0.492				0.378	0.372	0.259
$^tR(4,1)$	8128.280	-1.051	-0.270				0.627	0.604	0.007
$^tR(3,0)$	8162.653	-0.666	-0.257	-0.261	-0.780	-0.722	0.656	0.609	0.101
$^nR(2,1)$	8163.129	-0.166	-0.311	-0.310	-0.369	-0.721	0.587	0.612	0.158
Average (o-c)		-0.226	-0.334	-0.321	-0.253	-0.735		0.528	0.116
σ(o-c)		0.468	0.089	0.083	0.295	0.063		0.086	0.095
σ(o-c) [no J=0]		0.482	0.069	0.052	0.306	0.014		0.052	0.070

[a]: Transition key: this labeling $\{P|Q|R\}(J,G)$ is used by McCall and Oka [50], where P, Q, R is referred to $\Delta J = -1, 0, +1$ and J and G refer to the lower state of the transition. For further notation, see [50];

[b]: Author key: McCall, Oka (2000): [50], Wat = Watson (1996) [44], NMT = Neale, Miller, & Tennyson (1996) [45], Da = Dinelli *et al.* (adjusted potential)(1997) [46], WH = Wolniewicz & Hinze (1994) [70], Db = Dinelli *et al.* (*ab initio*) (1997) [46], J = Jaquet (2002) [30]; [c]: J: GGCIR12f: calculations with diagonal adiabatic corrections [30] (potential data from JCRK [27, 28] and CI-R12 with f-functions [30]; NU23 mass; [d] J: calculations with diagonal adiabatic corrections (potential data from JCRK [27,28]; adia: NU23 mass, non-ad: rotational and vibrational mass; without extra term in the kinetic energy (see [31])).

4.2 Combination band spectroscopy between 7785 and 8164 cm^{-1}

The analysis of observed spectra of H_3^+ has relied heavily on *ab initio* theory [106]. While the $\nu_2 \leftarrow 0$ fundamental band could be understood using perturbation theory, this was not the case for hot bands. Because the molecule is fairly floppy (small nuclear mass, highly anharmonic potential) different rovibrational states are strongly mixed. Variational calculations were needed for correct assignment. Statements of Bawendi *et al.* [107] that "probably the best strategy for H_3^+ is to provide the *ab initio* theorists with our experimentally determined energy levels so that they can further adjust .. their potentials and accurately predict new rovibrational transitions" is not valid anymore, at least for H_3^+. For the investigated frequency ranges so far, the prediction of rovibrational eigenstates and related transitions seems to be less problematic, the prediction whether the transition will be seen in the experimental setup, however, is. This point will be discussed in the following when we address the combination band spectroscopy in the region 7785 - 8164 cm^{-1} (Fig. 12.13). Within that energy region different rovibrational states are involved: $3\nu_2^3, \nu_1 2\nu_2^0, \nu_1 2\nu_2^2, 2\nu_1\nu_2^1$. The largest intensities are related to the transitions from the ground state to $\nu_1 2\nu_2^2$ and smaller intensities are related to $2\nu_1\nu_2^1 \leftarrow 0$. The different intensities for the region between 7785 and 8164 cm^{-1} are shown in Fig. 12.14 and calculated for an assumed temperature of the investigated gas/plasma of 300 K^o. In Table 12.8 a comparison of recent experimental work and variational calculations is presented (further detailed results, especially those transitions experimentally not seen so far in that frequency range, are given in [30]).

In recent years reliable potentials, (a) *ab initio* and (b) empirical potentials have been developed. In the case of empirically adjusted potentials (Wat, NMT, Da; based on *ab initio* fitting results and using available experimental data), the average difference values ($\Delta\nu$(obs.-calc.)) for the investigated frequency range lie between 0.23 and 0.33 cm^{-1}, with larger standard deviations for the earlier studies (Wat: 0.47 cm^{-1})

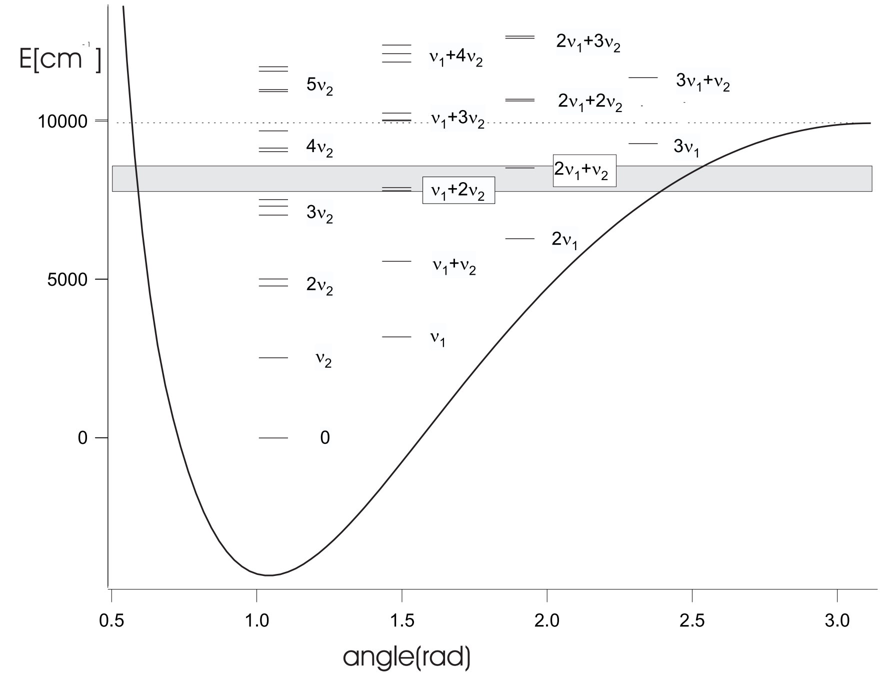

Figure 12.13. 1D representation of the potential energy curve of H_3^+ along the bending angle. Position of the vibrational energy levels (J=0) and the barrier to linearity is indicated. The shaded region indicates the frequency range of the transitions near 1.25 μm. (Adapted from B.J. McCall, Phil. Trans. R. Soc. Lond. A **358** (2000) 2385).

and smaller ones for the recent work (NMT, Da: 0.08 - 0.09 cm^{-1}). The latter accuracy was not possible to achieve before the first CI-R12 calculations became available (*e.g.* producing that part of the PES needed for spectroscopy [17]). In the case of *ab initio* potentials, Wolniewicz and Hinze (WH) (hyperspherical coordinate method) used the MBB-fit [16]. Their frequencies scatter around the experimental values with a resulting σ(o-c) of $\approx$ 0.3 cm^{-1}. Db use a potential that is based on the CI-R12 results of Röhse *et al.* [17] including diagonal adiabatic corrections (SCF quality). Polyansky and Tennyson's (PT) [31] results, presented in Ref. [50], are similar to ours in the second-last column (using our electronic potential with relativistic contributions and diagonal adiabatic corrections), but show deviations which are difficult to understand. This discrepancy might be related to the fact that PT refitted our *ab initio* data hoping to gain a more reliable fit. PT's σ(o-c) is twice as large as for our adiabatic calculations.

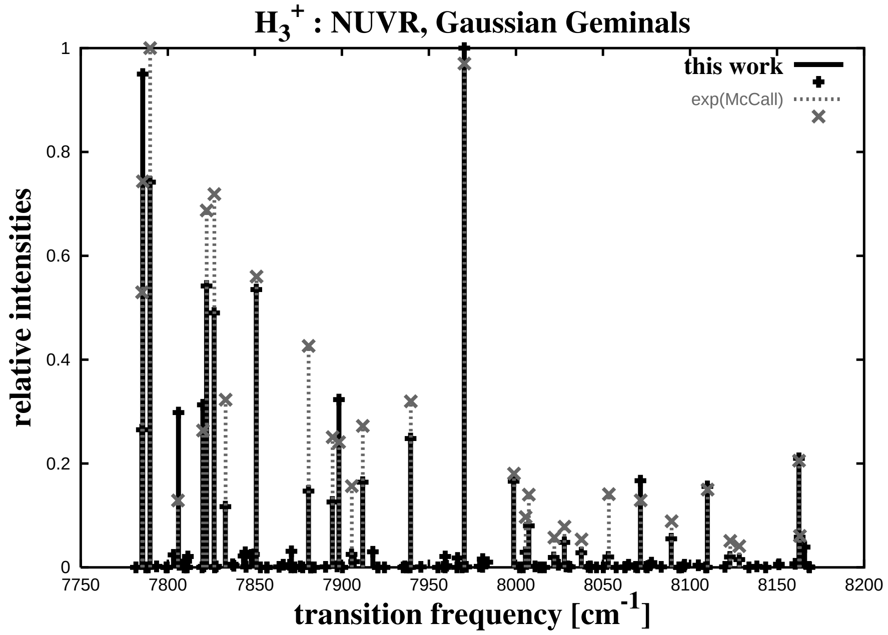

Figure 12.14. Combination band spectroscopy of H_3^+: 28 transitions of $\nu_1 + 2\nu_2^2 \leftarrow 0$ and two transitions of $2\nu_1 + \nu_2 \leftarrow 0$ near 1.25 μm. Comparison of experiment [50] with variational calculations. (See Table 12.8).

When trying to simulate non-adiabatic effects (using **NUVR**) we found a further reduction of the deviation to experiment. As one can see, for one transition (7805.893 cm^{-1}), the deviation is much smaller than the average, which is more or less constant within the given frequency range. The transition at 7805.893 cm^{-1} connects the ground state with a rotationless, vibrationally excited ($\nu_1 2\nu_2^2$) state. A good agreement to experiment was already expected for the calculation including only adiabatic corrections, because non-adiabatic effects should have minor contributions. Our simulation of non-adiabaticity using different masses for rotational and vibrational motion is too rough to keep the good result for that special transition and to improve only the other transitions; the deviation is of the same magnitude as before, but with changed sign. In addition, we compare observed and calculated relative intensities (Fig. 12.14); all calculated transitions with intensities higher than 1% of the reference peak are given (for details see Table 7 and 8 in [30]). Compared to experiment, we calculated 15 additional lines between 7802.9 and 8165.4 cm^{-1}. Probably these lines have not been detected so far, because they lie at the very limit of the sensitivity of the spectrometer, although theoretical and experimental intensities (see Fig. 12.14) deviate only in few cases by a factor larger than two.

5. H_3^+ and the barrier to linearity

As already mentioned before rovibrational eigenvalues calculated by Jaquet [30] using Jacobi coordinates and Schiffels and Alijah *et al.* [98] using hyperspherical coordinates can differ at energies near the barrier to linearity by more then 0.5 cm^{-1}. Small deviations are related to the fact that slightly different fits to the same ab initio data have been used. Larger deviations result from the fact that the TRIATOM-code (with Morse oscillator functions in the R-direction) is inadequate for regions where the Jacobi coordinate R tends to zero (i.e. barrier to linearity). New calculations with the DVR3DRJ-code (with spherical oscillator functions in the R-direction) are reproduced exactly by the hyperspherical coordinates code [70, 98] (we performed recently both calculations with exactly the same potential).

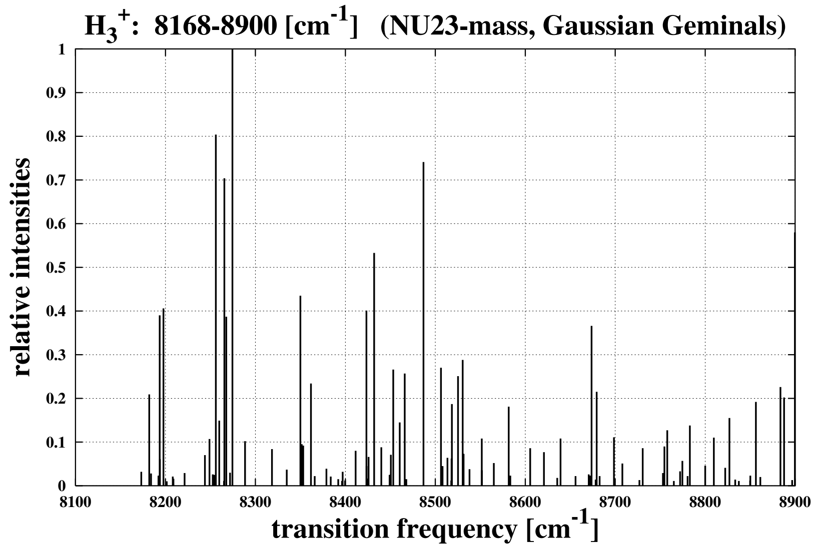

Figure 12.15. Combination band spectroscopy of H_3^+: 8168-8900 cm^{-1}. Transitions with intensities larger than 1% of the maximum intensity in the given frequency range; assumed temperature: $T = 300$ K^o. (Details: Table 12.9).

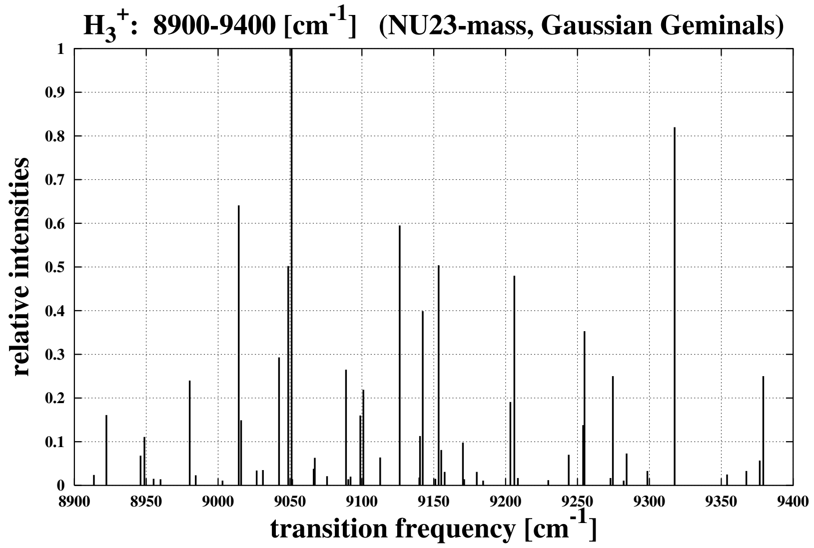

Figure 12.16. Combination band spectroscopy of H_3^+: 8900-9400 cm^{-1}. Transitions with intensities larger than 1% of the maximum intensity in the given frequency range; assumed temperature: $T = 300$ K^o. (Details: Table 12.10).

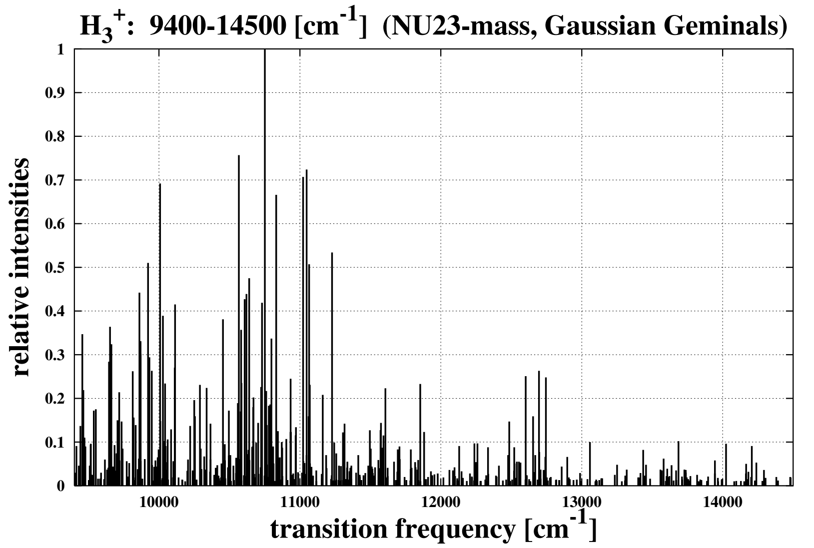

Figure 12.17. Combination band spectroscopy of H_3^+: 9400-14500 cm^{-1}. Transitions with intensities larger than 1% of the maximum intensity in the given frequency range; assumed temperature: $T = 300$ K^o. (Details: Table 12.11).

In the figures 12.15, 12.16, 12.17 and tables 12.9, 12.10, 12.11 we present new results of transitions above 8164 cm^{-1}, which have been calculated with TRIATOM: we are aware of some numerical problems for energies near the barrier to linearity; in the meantime new DVR3DRJ calculations are under the way to replace the present results. We compared our results with the data of Schiffels *at al.* [98] to get information about the reliability of the frequencies in various energy regions. In addition, one has to take into account, that the frequency calculations are based on a fit that is not strongly supported by sufficient *ab initio* data in the energy region above the barrier to linearity. Nonetheless, for the assumed temperature of $T = 300$ K^o the new presented results will propose experimentalist a reliable spectrum.

6. The reaction dynamics of H^+ and H_2

Charge transfer belongs to the broader class of collision processes involving transitions between two or more potential hypersurfaces. These transitions usually occur in well defined regions of configuration space where the diabatic potential energy surfaces cross and where the Born-Oppenheimer approximation breaks down. Such crossing processes occur in reactive or nonreative collisions of open shell systems and in most ion-molecule collisions [108].

For a theoretical study of such systems, a knowledge of the different PES's is required. The dynamics accounts for the transition from one surface to the next.

Representations of the lowest three electronic $^1A_1$ (C_{2v}) PESs (using the 'diatomics-in-molecules' method) and the associated first derivative non-adiabatic couplings are given in Fig. 12.5 and Fig. 12.6.

For the H^+ + H_2 system differential cross sections have been determined in a broad energy range [109] . The possible channels are

$H^+ + H_2(v_i = 0) \rightarrow H_3^+ \rightarrow H^+ + H_2(v_f), \quad \Delta E_{el} = 0,$

$H^+ + H_2(v_i = 0) \rightarrow H_3^+ \rightarrow H + H_2^+(v_f), \quad \Delta E_{el} = 1.83$ eV.

Preliminary wave packet investigations of the collision dynamics have already been performed [111] using the diatomic-in-molecules (DIM) potential. These scattering investigations will be of improved quality when the new global *ab initio* surfaces (GG combined with CI-R12) for the ground and electronically excited states become available.

Table 12.9. Transitions $\nu_1''\nu_2''^{l''}(J'',G'') \leftarrow 0'0'^{0'}(J',G')$ in the 8168-8900 cm^{-1} frequency range with more than 5% of the maximum relative intensity I_{rel} (potential: GG, basis set: 3000, mass: **NU23**). (Frequencies and term values in cm^{-1}).

	J"	G"	ν_1"	ν_2"	l"	J'	G'	E"	E'	Φ"	Φ'	I_{rel}
8182.048	3	3	2	1	1	4	3	8840.562	658.514	A_2'	A_2''	0.21
8193.670	4	1	1	2	2	4	4	8695.552	501.882	E"	E'	0.39
8193.927	5	1	1	2	2	5	4	9122.612	928.685	E"	E'	0.06
8197.835	3	4	2	1	1	4	4	8699.717	501.882	E"	E'	0.41
8243.949	2	0	2	1	1	3	0	8760.671	516.722	A_2''	A_2'	0.07
8248.923	2	1	2	1	1	3	1	8743.538	494.615	E'	E"	0.11
8256.054	4	2	1	2	2	3	1	8750.669	494.615	E'	E"	0.80
8259.789	2	2	2	1	1	3	2	8687.678	427.889	E"	E'	0.15
8265.489	3	1	1	2	2	2	2	8434.737	169.248	E"	E'	0.70
8267.663	4	1	1	2	2	3	2	8695.552	427.889	E"	E'	0.39
8274.462	2	3	2	1	1	3	3	8589.715	315.253	A_2'	A_2''	1.00
8288.557	5	2	1	2	2	5	5	9017.344	728.787	E'	E"	0.10
8318.428	5	0	1	2	0	4	3	8976.942	658.514	A_2'	A_2''	0.08
8350.036	1	2	2	1	1	2	2	8519.284	169.248	E"	E'	0.43
8351.530	5	2	1	2	2	4	1	9184.854	833.324	E'	E"	0.09
8353.134	6	3	1	2	2	5	0	9624.012	1270.878	A_2''	A_2'	0.09
8361.751	4	1	1	2	2	3	2	8789.640	427.889	E"	E'	0.23
8411.457	4	3	2	1	1	4	3	9069.971	658.514	A_2'	A_2''	0.08
8423.413	0	1	2	1	1	1	1	8487.518	64.105	E'	E"	0.40
8425.892	4	1	2	1	1	4	1	9259.216	833.324	E'	E"	0.07
8432.066	4	0	1	2	2	3	3	8747.319	315.253	A_2'	A_2''	0.53
8439.956	3	2	2	1	1	3	2	8867.845	427.889	E"	E'	0.09
8450.589	3	1	2	1	1	3	1	8945.204	494.615	E'	E"	0.07
8453.211	3	0	2	1	1	3	0	8969.933	516.722	A_2''	A_2'	0.27
8460.507	5	1	1	2	2	4	2	9228.744	768.237	E"	E'	0.14
8466.016	2	1	2	1	1	2	1	8703.299	237.283	E'	E"	0.26
8486.835	1	0	2	1	1	1	0	8573.770	86.935	A_2''	A_2'	0.74
8506.255	2	1	2	1	1	2	1	8743.538	237.283	E'	E"	0.27
8513.529	3	2	2	1	1	3	2	8941.418	427.889	E"	E'	0.06
8518.119	4	3	2	1	1	4	3	9176.633	658.514	A_2'	A_2''	0.06
8518.430	2	2	2	1	1	2	2	8687.678	169.248	E"	E'	0.19
8525.309	3	3	2	1	1	3	3	8840.562	315.253	A_2'	A_2''	0.25
8530.469	3	4	2	1	1	2	2	8699.717	169.248	E"	E'	0.29
8531.447	4	4	2	1	1	4	4	9033.329	501.882	E"	E'	0.07
8551.654	6	4	1	2	2	5	5	9280.441	728.787	E'	E"	0.11
8565.007	6	0	1	2	2	5	3	9645.161	1080.154	A_2'	A_2''	0.05
8581.597	5	0	1	2	2	4	3	9240.111	658.514	A_2'	A_2''	0.18
8605.440	4	4	2	1	1	3	2	9033.329	427.889	E"	E'	0.09
8620.730	5	1	1	2	2	4	4	9122.612	501.882	E"	E'	0.08
8639.194	2	1	2	1	1	1	1	8703.299	64.105	E'	E"	0.11
8673.736	2	0	2	1	1	1	0	8760.671	86.935	A_2''	A_2'	0.37
8679.433	2	1	2	1	1	1	1	8743.538	64.105	E'	E"	0.22
8698.597	3	2	2	1	1	2	2	8867.845	169.248	E"	E'	0.11
8707.921	3	1	2	1	1	2	1	8945.204	237.283	E'	E"	0.05
8730.309	4	4	0	4	0	5	5	9459.096	728.787	E'	E"	0.09
8754.718	4	3	2	1	1	3	3	9069.971	315.253	A_2'	A_2''	0.09
8757.555	5	3	0	4	2	6	6	9753.120	995.565	A_2''	A_2'	0.13
8774.577	3	3	0	4	0	3	0	9291.299	516.722	A_2''	A_2'	0.06
8782.842	4	6	0	4	2	4	3	9441.356	658.514	A_2'	A_2''	0.14
8809.559	3	5	0	4	2	4	4	9311.441	501.882	E"	E'	0.11
8826.983	3	0	0	4	0	4	3	9485.497	658.514	A_2'	A_2''	0.15
8856.081	4	2	0	4	0	5	5	9584.868	728.787	E'	E"	0.19
8883.552	3	5	0	4	2	3	2	9311.441	427.889	E"	E'	0.23
8887.761	2	3	0	4	2	3	0	9404.483	516.722	A_2''	A_2'	0.20
8899.705	1	1	0	4	0	2	2	9068.953	169.248	E"	E'	0.58

Table 12.10. Transitions $\nu_1''\nu_2''^{l''}(J'',G'') \leftarrow 0'0'^{0'}(J',G')$ in the 8900-9400 cm^{-1} frequency range with more than 1% of the maximum relative intensity I_{rel} (potential: GG, basis set: 3000, mass: **NU23**). (Frequencies and term values in cm^{-1}).

	J”	G”	ν_1”	ν_2”	l”	J’	G’	E”	E’	Φ”	Φ’	I_{rel}
8913.526	4	5	0	4	2	4	2	9681.763	768.237	E”	E’	0.02
8922.076	3	1	0	4	0	4	4	9423.958	501.882	E”	E’	0.16
8945.928	3	2	0	4	0	3	1	9440.543	494.615	E’	E”	0.07
8948.749	2	2	0	4	2	3	1	9443.364	494.615	E’	E”	0.11
8955.049	4	0	0	4	2	5	3	10035.203	1080.154	A_2'	A_2''	0.02
8959.913	4	4	0	4	2	4	1	9793.237	833.324	E’	E”	0.01
8980.145	2	4	0	4	2	2	1	9217.428	237.283	E’	E”	0.24
8984.316	1	2	0	4	2	2	1	9221.599	237.283	E’	E”	0.02
9003.031	7	0	0	0	0	6	6	9998.596	995.565	A_2''	A_2'	0.01
9014.293	2	0	0	4	2	3	3	9329.546	315.253	A_2'	A_2''	0.64
9015.980	2	1	0	4	2	3	2	9443.869	427.889	E”	E’	0.15
9026.802	3	4	0	4	2	3	1	9521.417	494.615	E’	E”	0.03
9031.089	7	0	0	0	0	6	6	10026.654	995.565	A_2''	A_2'	0.03
9042.335	1	1	0	4	2	2	2	9211.583	169.248	E”	E’	0.29
9048.750	0	2	0	4	2	1	1	9112.855	64.105	E’	E”	0.50
9051.078	1	3	0	4	2	1	0	9138.013	86.935	A_2''	A_2'	1.00
9051.523	4	1	0	4	2	5	4	9980.208	928.685	E”	E’	0.01
9066.403	3	1	0	4	2	4	4	9568.285	501.882	E”	E’	0.04
9067.397	6	0	0	0	0	5	5	9796.184	728.787	E’	E”	0.06
9075.748	4	2	0	4	2	4	1	9909.072	833.324	E’	E”	0.02
9088.949	3	3	0	4	2	3	0	9605.671	516.722	A_2''	A_2'	0.26
9090.253	4	2	0	4	0	3	1	9584.868	494.615	E’	E”	0.01
9092.080	2	2	0	4	0	2	2	9261.328	169.248	E”	E’	0.02
9098.778	5	5	0	4	0	4	4	9600.660	501.882	E”	E’	0.16
9101.036	2	2	0	4	0	1	1	9165.141	64.105	E’	E”	0.22
9112.727	3	0	0	4	2	4	3	9771.241	658.514	A_2'	A_2''	0.06
9126.103	4	6	0	4	2	3	3	9441.356	315.253	A_2'	A_2''	0.60
9139.861	7	0	0	0	0	6	6	10135.426	995.565	A_2''	A_2'	0.02
9140.396	3	1	0	4	2	3	2	9568.285	427.889	E”	E’	0.11
9142.193	3	5	0	4	2	2	2	9311.441	169.248	E”	E’	0.40
9151.048	5	3	0	4	2	6	6	10146.613	995.565	A_2''	A_2'	0.01
9153.323	2	4	0	4	2	1	1	9217.428	64.105	E’	E”	0.50
9154.997	5	7	0	4	2	4	4	9656.879	501.882	E”	E’	0.08
9157.494	1	2	0	4	2	1	1	9221.599	64.105	E’	E”	0.03
9170.244	3	0	0	4	0	3	3	9485.497	315.253	A_2'	A_2''	0.10
9171.127	4	3	0	4	0	3	0	9687.849	516.722	A_2''	A_2'	0.01
9179.881	4	5	0	4	2	4	4	9681.763	501.882	E”	E’	0.03
9183.970	5	4	0	4	0	5	5	9912.757	728.787	E’	E”	0.01
9203.260	3	2	0	4	0	2	1	9440.543	237.283	E’	E”	0.19
9206.081	2	2	0	4	2	2	1	9443.364	237.283	E’	E”	0.48
9208.785	6	0	0	0	0	5	5	9937.572	728.787	E’	E”	0.02
9229.682	4	5	1	3	1	5	5	9958.469	728.787	E’	E”	0.01
9243.720	5	6	0	4	2	4	3	9902.234	658.514	A_2'	A_2''	0.07
9253.874	4	5	0	4	2	3	2	9681.763	427.889	E”	E’	0.14
9254.710	3	1	0	4	0	2	2	9423.958	169.248	E”	E’	0.35
9272.732	6	0	0	0	0	5	4	10201.417	928.685	E”	E’	0.02
9274.621	2	1	0	4	2	2	2	9443.869	169.248	E”	E’	0.25
9282.114	5	1	0	4	2	5	4	10210.799	928.685	E”	E’	0.01
9284.134	3	4	0	4	2	2	1	9521.417	237.283	E’	E”	0.07
9298.622	4	4	0	4	2	3	1	9793.237	494.615	E’	E”	0.03
9317.548	2	3	0	4	2	1	0	9404.483	86.935	A_2''	A_2'	0.82
9353.993	3	1	0	4	2	3	2	9781.882	427.889	E”	E’	0.02
9367.426	4	2	0	4	2	4	1	10200.750	833.324	E’	E”	0.03
9376.689	4	0	0	4	2	4	3	10035.203	658.514	A_2'	A_2''	0.06
9379.259	2	2	0	4	2	1	1	9443.364	64.105	E’	E”	0.25

Table 12.11. Transitions $\nu_1''\nu_2''^{l''}(J'',G'') \leftarrow 0'0'^{0'}(J',G')$ in the 9400-13700 cm^{-1} frequency range with more than 10% of the maximum relative intensity I_{rel} (potential: GG, basis set: 3000, mass: **NU23**). (Frequencies and term values in cm^{-1}).

	J"	G"	ν_1"	ν_2"	l"	J'	G'	E"	E'	Φ"	Φ'	I_{rel}
9442.562	5	1	0	4	2	4	2	10210.799	768.237	E"	E'	0.14
9455.988	3	0	0	4	2	3	3	9771.241	315.253	A_2'	A_2''	0.35
9463.854	4	5	1	3	1	3	1	9958.469	494.615	E'	E"	0.22
9471.980	4	2	1	3	1	4	2	10240.217	768.237	E"	E'	0.11
9538.096	3	2	0	4	2	2	1	9775.379	237.283	E'	E"	0.17
9552.319	4	1	0	4	2	3	2	9980.208	427.889	E"	E'	0.17
9645.858	3	4	1	3	1	2	2	9815.106	169.248	E"	E'	0.28
9652.539	4	3	0	4	2	3	0	10169.261	516.722	A_2''	A_2'	0.36
9662.395	1	0	1	3	1	1	0	9749.330	86.935	A_2''	A_2'	0.32
9706.135	4	2	0	4	2	3	1	10200.750	494.615	E'	E"	0.15
9718.059	2	6	0	4	4	3	3	10033.312	315.253	A_2'	A_2''	0.21
9735.280	4	4	1	3	1	3	2	10163.169	427.889	E"	E'	0.15
9813.811	2	1	1	3	1	1	1	9877.916	64.105	E'	E"	0.26
9820.428	1	4	1	3	3	2	2	9989.676	169.248	E"	E'	0.16
9834.655	2	5	1	3	3	2	1	10071.938	237.283	E'	E"	0.14
9861.400	2	0	1	3	1	1	0	9948.335	86.935	A_2''	A_2'	0.44
9869.476	3	2	1	3	1	2	2	10038.724	169.248	E"	E'	0.33
9870.694	5	1	0	4	0	4	4	10372.576	501.882	E"	E'	0.30
9922.387	4	3	1	3	1	3	3	10237.640	315.253	A_2'	A_2''	0.51
9930.214	3	1	1	3	1	2	1	10167.497	237.283	E'	E"	0.13
9932.604	0	4	0	4	4	1	1	9996.709	64.105	E'	E"	0.29
9949.579	3	2	1	3	1	2	2	10118.827	169.248	E"	E'	0.26
10007.833	2	5	1	3	3	1	1	10071.938	64.105	E'	E"	0.69
10010.072	4	1	0	4	2	3	2	10437.961	427.889	E"	E'	0.15
10028.401	2	4	0	4	4	2	1	10265.684	237.283	E'	E"	0.39
10032.458	2	2	1	3	3	3	2	10460.347	427.889	E"	E'	0.10
10043.396	1	3	0	4	4	1	0	10130.331	86.935	A_2''	A_2'	0.23
10062.232	4	1	1	3	1	3	1	10556.847	494.615	E'	E"	0.11
10086.562	4	0	1	3	1	3	0	10603.284	516.722	A_2''	A_2'	0.13
10112.146	1	2	1	3	3	2	2	10281.394	169.248	E"	E'	0.27
10114.751	3	5	1	3	3	2	1	10352.034	237.283	E'	E"	0.41
10221.130	4	5	1	3	3	3	1	10715.745	494.615	E'	E"	0.14
10250.754	2	3	0	4	4	1	0	10337.689	86.935	A_2''	A_2'	0.20
10255.093	2	2	0	4	4	1	1	10319.198	64.105	E'	E"	0.16
10291.099	2	2	1	3	3	2	2	10460.347	169.248	E"	E'	0.23
10338.498	2	1	1	3	3	1	1	10402.603	64.105	E'	E"	0.22
10365.939	3	1	0	4	4	2	2	10535.187	169.248	E"	E'	0.14
10453.963	4	0	0	4	4	3	3	10769.216	315.253	A_2'	A_2''	0.38
10496.538	5	5	0	5	3	4	4	10998.420	501.882	E'	E'	0.17
10559.801	3	3	2	2	2	3	0	11076.523	516.722	A_2''	A_2'	0.19
10567.414	1	3	2	2	2	1	0	10654.349	86.935	A_2''	A_2'	0.76
10580.415	0	2	2	2	2	1	1	10644.520	64.105	E'	E"	0.17
10582.853	2	0	2	2	2	3	3	10898.106	315.253	A_2'	A_2''	0.36
10585.669	1	1	2	2	2	2	2	10754.917	169.248	E"	E'	0.24
10608.453	4	6	2	2	2	3	3	10923.706	315.253	A_2'	A_2''	0.43
10620.887	3	5	2	2	2	2	2	10790.135	169.248	E"	E'	0.44
10640.209	2	4	2	2	2	1	1	10704.314	64.105	E'	E"	0.48
10668.959	1	2	2	2	2	1	1	10733.064	64.105	E'	E"	0.18
10670.988	2	2	2	2	2	2	1	10908.271	237.283	E'	E"	0.20
10704.335	4	5	2	2	2	3	2	11132.224	427.889	E"	E'	0.14
10725.104	3	4	2	2	2	2	1	10962.387	237.283	E'	E"	0.23
10730.925	2	3	0	5	1	3	3	11046.178	315.253	A_2'	A_2''	0.42
10751.276	2	3	2	2	2	1	0	10838.211	86.935	A_2''	A_2'	1.00
10758.823	1	2	0	5	1	2	2	10928.071	169.248	E"	E'	0.22

Table 12.11: (Continued)

10765.199	2	1	2	2	2	2	2	10934.447	169.248	E”	E’	0.14
10779.315	3	2	0	5	1	3	2	11207.204	427.889	E”	E’	0.18
10789.504	2	5	0	5	3	2	1	11026.787	237.283	E’	E”	0.19
10798.348	0	1	0	5	1	1	1	10862.453	64.105	E’	E”	0.34
10832.104	1	0	0	5	1	1	0	10919.039	86.935	A_2''	A_2'	0.67
10844.166	2	2	2	2	2	1	1	10908.271	64.105	E’	E”	0.12
10903.331	2	4	0	5	3	3	2	11331.220	427.889	E”	E’	0.11
10933.465	3	2	2	2	2	2	1	11170.748	237.283	E’	E”	0.12
10934.690	4	3	2	2	2	3	0	11451.412	516.722	A_2''	A_2'	0.24
10935.364	3	0	0	5	1	3	0	11452.086	516.722	A_2''	A_2'	0.12
10969.269	3	3	0	5	1	3	3	11284.522	315.253	A_2'	A_2''	0.12
10970.745	3	4	0	5	1	2	2	11139.993	169.248	E”	E’	0.13
11021.447	3	1	2	2	2	2	2	11190.695	169.248	E”	E’	0.71
11046.462	2	1	0	5	1	1	1	11110.567	64.105	E’	E”	0.72
11059.743	4	3	0	5	1	3	3	11374.996	315.253	A_2'	A_2''	0.51
11062.501	4	1	2	2	2	3	2	11490.390	427.889	E”	E’	0.16
11070.523	2	1	0	5	1	2	1	11307.806	237.283	E’	E”	0.23
11161.972	2	4	0	5	3	2	2	11331.220	169.248	E”	E’	0.21
11228.018	2	0	0	5	1	1	0	11314.953	86.935	A_2''	A_2'	0.53
11305.459	3	2	0	5	1	2	2	11474.707	169.248	E”	E’	0.12
11317.284	1	0	3	1	1	1	0	11404.219	86.935	A_2''	A_2'	0.14
11496.096	3	1	0	5	1	2	1	11733.379	237.283	E’	E”	0.13
11571.790	2	3	0	5	5	3	3	11887.043	315.253	A_2'	A_2''	0.13
11575.445	4	3	0	5	1	3	3	11890.698	315.253	A_2'	A_2''	0.14
11593.570	0	5	0	5	5	1	1	11657.675	64.105	E’	E”	0.12
11606.443	1	6	0	5	5	1	0	11693.378	86.935	A_2''	A_2'	0.22
11853.754	2	6	0	5	5	1	0	11940.689	86.935	A_2''	A_2'	0.23
11881.537	2	2	1	4	0	1	1	11945.642	64.105	E’	E”	0.12
12471.200	1	0	0	0	0	1	0	12558.135	86.935	A_2''	A_2'	0.15
12602.041	1	0	0	0	0	1	0	12688.976	86.935	A_2''	A_2'	0.25
12643.981	3	0	0	0	0	2	2	12813.229	169.248	E”	E’	0.16
12691.809	2	4	1	4	4	1	1	12755.914	64.105	E’	E”	0.26
12745.362	2	0	0	0	0	1	0	12832.297	86.935	A_2''	A_2'	0.25
13685.903	2	0	0	0	0	1	0	13772.838	86.935	A_2''	A_2'	0.10

7. Conclusions

In this overview we report on *ab initio* calculations of the rovibrational spectrum of a polyatomic molecule, based on a ”sub-wavenumber” accuracy potential energy surface, where besides the calculations of the electronic contributions to the BO-energy in addition relativistic effects and adiabatic contributions are included. The computed rovibronic frequencies agree with the experiment within ≈ 0.3 cm^{-1} for H_3^+ and ≈ 0.1 cm^{-1} for D_3^+. An accuracy for the spectroscopy of a triatomic molecule, for which the BO description is not sufficient, is reached, that has been achieved up to now only for H_2. The remaining discrepancy is due to nonadiabatic contributions which in the case of H_3^+ are smaller than in the case of H_2.

Further work is needed to include in the rovibrational calculations contributions to non-adiabaticity explicitly. It was shown by us that non-adiabatic effects can be simulated by using the appropriate masses, i.e. atomic masses for vibrational motion and nuclear mass for rotational motion, and that spectroscopic accuracy for most of the known transitions frequencies in the lower energy regime of the potential energy surface can be reached. The deviation to experiment is in the range of a *few hundredths of a wavenumber*.

The chosen atomic and nuclear masses are universal and can be used in other polyatomic hydrogenic systems, if e.g. for spectroscopic problems high accuracy has to be achieved. These calculations are then performed under the assumption that the potential energy surface and the adiabatic corrections are of high accuracy itself. It is clear that one can find optimal masses for each frequency band, but this was not our aim. The procedure which we proposed can be used for any system, if the deviation depends on the correct description of the nuclear motion of hydrogen.

In the present work it is shown that various methods are available to fit potential energy surfaces for a local or global representation. In the most recent work we calculated new *ab initio* points on different levels of accuracy (CI-R12 and full CI) for configurations far beyond the minimum energy region. With these data new fits have been performed using a polynomial expansion and the reproducing kernel Hilbert space method. For these new configurations we supplied new diagonal adiabatic corrections calculated on full CI level. The resulting new potential energy surfaces have already been used for calculating transition frequencies related to eigenstates below and above the barrier to linearity. They will be used in future work to extend the analysis of the spectrum of H_3^+ and its isotopomers to the higher frequency regime. Additional calculations using hyperspherical coordinate methods have already been started to clarify numerical problems for the energy regime near the barrier to linearity. In the case of H_3^+ we have seen that for highly accurate *ab initio* calculations it is difficult to keep the accuracy within the fit. New functional forms, fitting the complex topology of the adiabatic and non-adiabatic couplings, are needed.

Work is now in progress to solve the general eigenvalue problem by including non-adiabatic coupling matrix elements [32] between different low lying electronic states in H_3^+ to clarify spectroscopic problems. In addition, these coupling matrix elements will allow us to describe charge transfer processes in the reaction dynamics of $H^+ + H_2 \rightarrow H + H_2^+$ [110].

Acknowledgements: The author thanks W. Kutzelnigg, W. Cencek, J. Rychlewski, W. Klopper, and R. Röhse for a fruitful collaboration within the COST D9/13 project. Thanks to V. Staemmler, A. Alijah, B.J. McCall, C.M. Lindsay, T. Oka, and P. Kuntz for many stimulating discussions. The contribution of R. Röhse for providing the code for the adiabatic and non-adiabatic coupling elements is gratefully acknowledged. Thanks to A. Alijah making the hyperspherical coordinate code available to us.

References

[1] J. J. Thomson, *Phil. Mag.* **83**, 225 (1911).

[2] C. A. Coulson, *Proc. Camb. Phil. Soc.* **31**, 244 (1935).

[3] T. Oka, *Phil. Trans. R. Soc. Lond. A***358**, 2363 (2000).

[4] E. Herbst, S. Miller, T. Oka, and J. K. G. Watson (Eds.), The Royal Society Discussion Meeting on Astronomy, Physics, and Chemistry of H_3^+, *Phil. Trans. R. Soc. Lond. A***358**, 2359-2559 (2000).

[5] R. E. Cristofferson, S. Hagstrom, and F. Prosser, *J. Chem. Phys.* **40**, 236 (1964).

[6] H. Conroy, *J. Chem. Phys.* **40**, 603 (1964).

[7] G. D. Carney and R. N. Porter, *J. Chem. Phys.* **60**, 4521 (1974); **65**, 3547 (1976).

[8] J. K. G. Watson, *J. Mol. Struct.* **103**, 350 (1984).

[9] J. K. G. Watson, *Phil. Trans. R. Soc. Lond. A***358**, 2371 (2000).

[10] B. T. Sutcliffe and J. Tennyson, *J. Chem. Soc. Faraday Trans.* **83**, 1663 (1987).

[11] T. Oka, *Phys. Rev. Lett.* **45**, 531 (1980).

[12] B. J. McCall, *Phil. Trans. R. Soc. Lond. A***358**, 2385 (2000).

[13] S. Miller and J. Tennyson, *Chem. Soc. Rev.* **21**, 281 (1992).

[14] R. Röhse and W. Klopper, W. Kutzelnigg, *J. Chem. Phys.* **99**, 8830 (1993).

[15] J. B. Anderson, *J. Chem. Phys.* **96**, 307 (1992).

[16] W. Meyer, P. Botschwina, and P. G. Burton, *J. Chem. Phys.* **84**, 891 (1986).

[17] R. Röhse, W. Kutzelnigg, R. Jaquet, and W. Klopper, *J. Chem. Phys.* **101**, 2231 (1994).

[18] R. Jaquet and R. Röhse, *Mol. Phys.* **84**, 291 (1995).

[19] W. Kutzelnigg, *Theor. Chim. Acta.* **68**, 445 (1985).

[20] W. Kutzelnigg and W. Klopper, *J. Chem. Phys.* **94**, 1985 (1991).

[21] O. L. Polyansky, B. M. Dinelli, C. R. Le Sueur, and J. Tennyson, *J. Chem. Phys.* **102**, 9322 (1995).

[22] B. M. Dinelli, C. R. Le Sueur, J. Tennyson, and R. D. Amos, *Chem. Phys. Lett.* **232**, 295 (1995).

[23] B. M. Dinelli, S. Miller, and J. Tennyson, *J. Mol. Spectr.* **163**, 71 (1994).

[24] J. Tennyson and O. L. Polyansky, *Phys. Rev. A.* **50**, 314 (1994).

[25] B. M. Dinelli, O. L. Polyansky, and J. Tennyson, *J. Chem. Phys.* **103**, 10433 (1995).

[26] B. M. Dinelli, L. Neale, O. L. Polyansky, and J. Tennyson, *J. Mol. Spectr.* **181**, 142 (1997).

[27] W. Cencek, J. Rychlewski, R. Jaquet, and W. Kutzelnigg, *J. Chem. Phys.* **108**, 2831 (1998).

[28] R. Jaquet, W. Cencek, W. Kutzelnigg, and J. Rychlewski, *J. Chem. Phys.* **108**, 2837 (1998).

[29] R. Jaquet, *Chem. Phys. Lett.* **302**, 27 (1999).

[30] R. Jaquet, *Spectrochimica Acta A***58**, 691 (2002).

[31] O. L. Polyansky and J. Tennyson, *J. Chem. Phys.* **110**, 5056 (1999).

[32] R. Röhse and R. Jaquet, adiabatic and non- adiabatic coupling elements for H_3^+ with FULL-CI (*i. e.* the CI-R12 program, where the R12-part is switched off), unpublished results (1999).

[33] A. Carrington, I. R. McNab, and Y. D. West, *Mol. Phys.* **98**, 1073 (1993).

[34] I. R. McNab, *Adv. Chem. Phys.* **98**, 1 (1994).

[35] F. Kemp, C. E. Krik, and I. R. McNab, *Phil. Trans. R. Soc. Lond. A***358**, 2403 (2000).

[36] W. Cencek, J. Komasa, and J. Rychlewski, *Chem. Phys. Lett.* **246**, 417 (1995).

[37] G. C. Lie and D. Frye, *J. Chem. Phys.* **96**, 6784 (1992).

[38] G. D. Carney, and R. N. Porter, *Phys. Rev. Lett.* **45**, 537 (1980).

[39] C. Sanz, O. Roncero, C. Tablero, A. Aguado, and M. Paniagua, *J. Chem. Phys.* **114**, 2184 (2001).

[40] O. Friedrich, A. Alijah, Z. Xu, and A. J. C. Varandas, *Phys. Rev. Lett.* **86**, 1183 (2001).

[41] O. L. Polyansky, R. Prosmiti, W. Klopper, and J. Tennyson, *Mol. Phys.* **98**, 261 (2000).

[42] R. Prosmiti, O. L. Polyansky, and J. Tennyson, *Chem. Phys. Lett.* **273**, 107 (1997).

[43] A. Aguado, O. Roncero, C. Tablero, C. Sanz, and M. Paniagua, *J. Chem. Phys.* **112**, 1240 (2000).

[44] J. K. G. Watson, cited in Table 2 in [50].

[45] L. Neale, S. Miller, and J. Tennyson, *Astrophys. J.* **464**, 516 (1996).

[46] B. M. Dinelli, L. Neale, O. L. Polyansky, and J. Tennyson, *J. Mol. Spectr.* **181**, 142 (1997).

[47] J. C. Tully and P. K. Preston, *J. Chem. Phys.* **55** (1971) 562; **54**, 4297 (1971).

[48] P. J. Kuntz, in *The concept of the chemical bond*, edited by Z. B. Maksic, (Springer, Berlin, 1993), p. 321.

[49] F. A. Gianturco and F. Schneider, *Adv. Chem. Phys.* **82**, 135 (1992).

[50] B. J. McCall and T. Oka, *J. Chem. Phys.* **113**, 3104 (2000).

[51] C. M. Lindsay and B. J. McCall, *J. Mol. Spectr.* **210**, 60 (2001).

[52] B. J. McCall, PhD-thesis, Dep. of Chemistry, (University of Chicago, 2001).

[53] G. C. Schatz, *Rev. Mod. Phys.* **61**, 669 (1989).

[54] D. J. Searles and E. I. von Nagy-Felsobuki, *Ab initio variational calculations of molecular vibrational rotational spectra*, Lecture Notes in Chemistry **61**, (Springer, Berlin, 1993).

[55] A. J. C. Varandas, *Adv. Chem. Phys.* **74**, 255 (1988).

[56] P. G. Mezey, *Potential energy hypersurfaces*, (Elsevier, Amsterdam, 1987).

[57] M. M. Law and J. M. Hutson, *Comput. Phys. Commun.* **102**, 252 (1997).

[58] J. N. Murrell, S. Carter, S. C. Farantos, P. Huxley, and A. J. C. Varandas, *Molecular potential energy functions*, (Wiley, Brisbane, 1984).

[59] R. Jaquet, in *Potential Energy Surfaces*, edited by A. Sax, *Lecture Notes in Chemistry*, (Springer, Berlin, 1999), **71**, p. 95.

[60] T. S. Ho and H. Rabitz, *J. Chem. Phys.* **104**, 2584 (1996).

[61] P. G. Burton, E. I. von Nagy-Felsobuki, G. Doherty, and M. Hamilton, *Mol. Phys.* **55**, 527 (1985).

[62] A. Ichihara and K. Yokoyama, *J. Chem. Phys.* **103**, 2109 (1995).

[63] W. Klopper and W. Kutzelnigg, *Chem. Phys. Lett.* **134**, 17 (1987).

[64] W. Klopper and R. Röhse, *Theor. Chim. Acta.* **83**, 441 (1992).

[65] J. Rychlewski, W. Cencek, J. Komasa, *Chem. Phys. Lett.* **229**, 657 (1994).

[66] R. J. Gdanitz and R. Röhse, *Int. J. Quant. Chem.* **55**, 147 (1995); **59**, 505 (1996).

[67] R. Röhse and R. Jaquet, CI-R12 calculations for H_3^+ for additional points far above the barrier to linearity and in the asymptotic (H^+ + H_2) region, without f-functions, unpublished results (1999).

[68] DALTON, an *ab initio* electronic structure program, Release 1.0 (1997), written by T. Helgaker, H. J. Aa. Jensen, P. Jørgensen, J. Olsen, K. Ruud, H. Ågren, T. Andersen, K. L. Bak, V. Bakken, O. Christiansen, P. Dahle, E. K. Dalskov, T. Enevoldsen, B. Fernandez, H. Heiberg, H. Hettema, D. Jonsson, S. Kirpekar, R. Kobayashi, H. Koch, K. V. Mikkelsen, P. Norman, M. J. Packer, T. Saue, P. R. Taylor, and O. Vahtras.

[69] J. D. Augspurger and C. E. Dykstra, *J. Chem. Phys.* **88**, 3817 (1988).

[70] L. Wolniewicz and J. Hinze, *J. Chem. Phys.* **101**, 9817 (1994).

[71] R. T. Pack and G. A. Parker, *J. Chem. Phys.* **87**, 3888 (1987).

[72] N. C. Handy, Y. Yamaguchi, and H. F. Schaefer III, *J. Chem. Phys.* **84**, 4481 (1986).

[73] A. G. Ioannou, R. D. Amos, and N. C. Handy, *Chem. Phys. Lett.* **251**, 52 (1996).

[74] N. C. Handy and A. M. Lee, *Chem. Phys. Lett.* **252**, 425 (1996).

[75] M. Born and K. Huang, *Dynamical theory of crystal lattices* (Oxford Unversity Press, New York, 1956).

[76] R. D. Bardo and M. Wolfsberg, *J. Chem. Phys.* **68**, 2686 (1978).

[77] W. Kutzelnigg, *Mol. Phys.* **90**, 909 (1997).

[78] J. K. G. Watson, *J. Mol. Spectr.* **45**, 99 (1973).

[79] J. K. G. Watson, *J. Mol. Spectr.* **80**, 411 (1980).

[80] R. M. Herman and A. Asgharian, *J. Mol. Spectr.* **19**, 305 (1964).

[81] J. Tennyson, in *Computational Molecular Spectroscopy*, edited by P. Jensen and P. R. Bunker (Wiley, 2000), p. 305.

[82] B. T. Sutcliffe and J. Tennyson, *Int. J. Quant. Chem.* **29**, 183 (1991).

[83] J. Tennyson and B. T. Sutcliffe, *Mol. Phys.* **51**, 887 (1984).

[84] J. Tennyson and S. Miller, *Comput. Phys. Commun.* **55**, 149 (1989).

[85] R. Jaquet, program package FEMEIG, 3D eigenvalue solver of bound and quasi-bound problems using finite elements methods, unpublished (1997).

[86] R. Jaquet, A. Kumpf, and M. Heinen, *J. Chem. Soc. Faraday Trans.* **93**, 1027 (1997).

[87] A. Kumpf, PhD-thesis, Dep. of Chemistry, (University Siegen, 1999).

[88] R. Jaquet, *Comput. Phys. Commun.* **58**, 257 (1990).

[89] S. Miller and J. Tennyson, *J. Mol. Spectr.* **128**, 183 (1987).

[90] M. Quack, *Mol. Phys.* **34**, 477 (1977).

[91] R. E. Moss, *Mol. Phys.* **89**, 195 (1996).

[92] P. R. Bunker and R. E. Moss, *Mol. Phys.* **33**, 417 (1977).

[93] M. A. Kostin, O. L. Polyansky, and J. Tennyson, *J. Chem. Phys.* **116**, 7564 (2002).

[94] A. Alijah, J. Hinze, and L. Wolniewicz, *Mol. Phys.* **85**, 1105 (1995).

[95] A. Alijah, L. Wolniewicz, and J. Hinze, *Mol. Phys.* **85**, 1125 (1995).

[96] A. Alijah and M. Beuger, *Mol. Phys.* **88**, 497 (1996).

[97] J. Hinze, A. Alijah, and L. Wolniewicz, *Polish J. Chem.***72**, 1293 (1998).

[98] P. Schiffels, A. Alijah, and J. Hinze, *Mol. Phys.* (2002, submitted), part I and II.

[99] L. Kao, T. Oka, S. Miller, and J. Tennyson, *Astrophys. J. Suppl. Ser.* **77**, 317 (1991).

[100] S. C. Foster, A. R. W. McKellar, I. R. Peterkin, J. K. G. Watson, F. S. Pan, M. W. Crofton, R. S. Altman, and T. Oka, *J. Chem. Phys.* **84**, 91 (1985).

[101] I. N. Kozin, O. L. Polyansky, and N. F. Zobov, *J. Mol. Spectr.* **128**, 126 (1988).

[102] O. L. Polyansky, and A. R. W. McKellar, *J. Chem. Phys.* **92**, 4039 (1990).

[103] J. T. Shy, J. W. Farley, W. E. Lamb, and W. H. Wing, *Phys. Rev. Lett.* **45**, 535 (1980).

[104] R. Jaquet and A. Alijah, comparison of eigenvalues for H_3^+ based on calculations with hyperspherical and Jacobi coordinates.

[105] J. Tennyson, J. R. Henderson, and N. G. Fulton, *Comput. Phys. Commun.* **86**, 175 (1995).

[106] J. Tennyson, *Rep. Prog. Phys.* **57**, 421 (1995).

[107] M. G. Bawendi, B. D. Rehfus, and T. Oka, *J. Chem. Phys.* **93**, 6200 (1990).

[108] M. Baer, G. Niedner-Schattenburg, and J. P. Toennies, *J. Chem. Phys.* **91**, 4169 (1989).

[109] G. Niedner, M. Noll, and J. P. Toennies, *J. Chem. Phys.* **87**, 2685 (1987).

[110] R. Jaquet and C. Morari, wave packet calculations, unpublished (2001).

[111] C. Morari, PhD-thesis, Dep. of Chemistry, (University Siegen, 2001).